AFRL-IF-RS-TR-2003-304
Final Technical Report
January 2004

SCALING RELATIONSHIPS FOR BIOMOLECULES ADHESION AND ACTIVITY ON POLYMERIC SURFACES

Iris, Swinburne University of Technology

Sponsored by
Defense Advanced Research Projects Agency
DARPA Order No. J406

AIR FORCE RESEARCH LABORATORY
INFORMATION DIRECTORATE
ROME RESEARCH SITE
ROME, NEW YORK

STINFO FINAL REPORT

This report has been reviewed by the Air Force Research Laboratory, Information Directorate, Public Affairs Office (IFOIPA) and is releasable to the National Technical Information Service (NTIS). At NTIS it will be releasable to the general public, including foreign nations.

AFRL-IF-RS-TR-2003-304 has been reviewed and is approved for publication.

APPROVED: /s/

DUANE GILMOUR
Project Engineer

FOR THE DIRECTOR: /s/

JAMES A. COLLINS, Acting Chief
Information Technology Division
Information Directorate

REPORT DOCUMENTATION PAGE

Form Approved
OMB No. 074-0188

1. AGENCY USE ONLY (Leave blank)	2. REPORT DATE	3. REPORT TYPE AND DATES COVERED
	JANUARY 2004	Final Jul 00 – Jul 03

4. TITLE AND SUBTITLE
SCALING RELATIONSHIPS FOR BIOMOLECULES ADHESION AND ACTIVITY ON POLYMERIC SURFACES

5. FUNDING NUMBERS
C - F30602-00-2-0614
PE - 61101E
PR - E117
TA - 00
WU - 65

6. AUTHOR(S)
Dan Nicolau and Sverre Myhra

7. PERFORMING ORGANIZATION NAME(S) AND ADDRESS(ES)
Iris, Swinburne University of Technology
PO Box 318
Hawthorne Victoria 3122 Australia

8. PERFORMING ORGANIZATION REPORT NUMBER
N/A

9. SPONSORING / MONITORING AGENCY NAME(S) AND ADDRESS(ES)
Defense Advanced Research Project Agency
3701 North Fairfax Drive
Arlington Virginia 22203-1714

AFRL/IFTC
26 Electronic Parkway
Rome New York 13441-4514

10. SPONSORING / MONITORING AGENCY REPORT NUMBER
AFRL-IF-RS-TR-2003-304

11. SUPPLEMENTARY NOTES
AFRL Project Engineer: Duane Gilmour/IFTC/(315) 330-3550/ Duane.Gilmour@rl.af.mil

12a. DISTRIBUTION / AVAILABILITY STATEMENT
APPROVED FOR PUBLIC RELEASE; DISTRIBUTION UNLIMITED.

12b. DISTRIBUTION CODE

13. ABSTRACT *(Maximum 200 Words)*
The project focused on the understanding and engineering quantification of the attachment of biomolecules and cells on polymeric surfaces. The project delivered design tools and guidelines that can be used in the process of design, fabrication and operation of microfluidics devices, in particular plastic-based devices. The project comprised modeling/simulation and experimental modules. The classification results are contained in an online freely accessible database, http://www.bionanoeng.com/bad. This biomolecular adsorption database has over 500 entries, and has been utilized by -1000 clients/month (40% edu, 30% com & 20% gov). A modeling capability for protein adsorption on polymeric surfaces has also been developed. Experiments, based on atomic force microscopy, were conducted to measure forces between biomolecules. The database, combined with the experimental results and the modeling capability will allow for improved design of microfluidic devices.

14. SUBJECT TERMS
Microfluidic Device, AFM, Atomic Force Microscopy, Polymer Microchannels, Polymer Surface, Protein Adsorption, Biomolecule Adhesion, Biomolecule Adsorption,

15. NUMBER OF PAGES
50

16. PRICE CODE

17. SECURITY CLASSIFICATION OF REPORT	18. SECURITY CLASSIFICATION OF THIS PAGE	19. SECURITY CLASSIFICATION OF ABSTRACT	20. LIMITATION OF ABSTRACT
UNCLASSIFIED	UNCLASSIFIED	UNCLASSIFIED	UL

TABLE OF CONTENTS

LIST OF FIGURES

LIST OF TABLES

ACKNOWLEDGEMENTS

The PI's specifically acknowledge the partial support of The Australian Research Council and of the Cooperative Research Centre for Microtechnology, which contributed with funds to support several students during the period of this project.

The PI's wish to express their gratitude to Dr. Anantha Krishnan, who took the time to understand all aspects of the project and suggested the redirection of research to 'greener pastures'.

The PIs also wish to thank their colleagues, postdoctoral fellows, and research students who contributed to the research reported here. Without any particular order, other than alphabetical, these thanks go to Ms. Yulia Alexeeva, Ms. Yolanta Blach, Dr. Jinan Cao, Ms. Luisa Filipponi, Mr. Florin Fulga, A/Prof. Elena Ivanova, Mr. Dan Nicolau Jr., Ms. Anna Oliveira, Mr. Michal Paperinik, Dr. Duy Pham, Dr. Livia Tonge, Mr. Andrea Viezolli, Dr. Greg Watson, and Dr. Jon Wright.

The first PI wants to thank many in the Simbiosys and Bioflips community for numerous insightful discussions. In particular to Dr. Piotr Grodzinski from Motorola (now at Los Alamos Labs) and his team; Prof. Jay Hicks from Clemson and his team; Dr. Andrzej Przekwas from CFDRC; Dr. David Clague from Lawrence Livermore Labs; for quasi-formal collaborations.

The co-PI's want to thank Swinburne University of Technology and Griffith University, their respective institutions, for providing much of the research infrastructure as well as constant help with financial and legal matters. Special thanks go to Peter Hotchin and Liz Jolley; and Brian Smith, from Swinburne and Griffith, respectively; and to Drs. Bruce Whan and Seth Jones from Swinburne Knowledge for work towards commercialization of a patent resulting from this grant.

The first PI wishes to express his appreciation towards Duane Gilmour and Clare Thiem, who constantly monitored the progress of the research and helped in keeping it on track. DARPA Simbiosys ultra-friendly team, 'people behind the scenes' such as Steve Kenney; Carol Higgins, and Nanette Rushing (apologies if I missed someone) who supported us before, during and after the PI meetings with style, poise and dedication.

Dr. Tom Spurling, the Director of Industrial Research Institute had a particularly critical input in the second half of the grant – the first PI wants to acknowledge his help.

Finally, the first PI wishes to express his special thanks towards the (outgoing) Vice-Chancellor of Swinburne University, Prof. Iain Wallace, for his critical assistance and encouragement at the beginning of the grant and for his constant attention during the period of the grant. Without Iain much of the achievements reported here would not have been possible.

1.0 EXECUTIVE SUMMARY

The project "SCALING RELATIONSHIPS FOR BIOMOLECULES ADHESION AND ACTIVITY ON POLYMERIC SURFACES" has focused on the understanding and engineering quantification of the attachment of biomolecules and cells on polymeric surfaces. The project aims to deliver design tools and guidelines that can be used in the process of design, fabrication and operation of microfluidics devices, in particular plastic-based devices. The project comprised modeling/simulation and experimental modules as summarized in the following sections.

MODELING/SIMULATION MODULE

Quantification of the adsorption-specific descriptors of biomolecules.
The biomolecular surface, in particular proteins, has been described in the context of biomolecule-biomolecule recognition and not in the context of biomolecule-surface adsorption. Biomolecule adsorption poses difficult quantification problems for the distribution of hydrophobicity and charges, because only a 'leopard-like' area on the biomolecular surface contributes to adsorption on flat surfaces. To that end, we developed new methods for the classification of proteins based on the quantification of their adsorption-relevant molecular descriptors.

Biomolecular adsorption database (BAD).
BAD (http://www.bionanoeng.com/bad) comprises a few hundred cases of protein adsorption on different materials and technological conditions. The molecular descriptors regarding the protein are calculated with an in-house developed software package. The site has been used by many thousands of researchers and is visited a few hundred times per week (over the period of the last 2 years).

Scaling relationships for protein adsorption.
The key deliverable of the project has been the predictive scaling relationships regarding biomolecule adsorption on polymeric surfaces that directly link the height of the adsorbed biomolecular layer to (i) molecular descriptors of the adsorbed biomolecule; (ii) environment conditions; and (iii) surface descriptors. The predictive power reached 80-90% correlation fit, depending on the range of variables.

Impact. The quantification of adsorption-relevant descriptors allows the estimation of biomolecular adsorption if similar experiments are available, greatly reducing the experimental work and design effort; and it can be also used for the rational design of bioactive nano-structured surfaces. BAD can be used, in conjunction with the clustering and descriptors software for the estimation of biomolecular adsorption. The predictive relationships, which are ready-to-use, also proved that protein adsorption has an insignificant impact (resulting in much simpler design and operation) for microfluidics devices with channels larger than 1.5-2 μm.

EXPERIMENTAL MODULE

Atomic Force Microscopy studies on bioactivity of biomolecular and cellular layers.
Atomic Force Microscopy (AFM) was used to analyze biomolecular and cellular films on polymers. Firstly, AFM measured the attraction/repulsion forces between 'model' amino-acids mounted on an AFM tip and 'model' surfaces. These forces are critical inputs to a fundamental model of biomolecular adsorption. Secondly, AFM studies proved that the polymer surface modulates the molecular structure of the DNA molecules and hence the hybridization process. Thirdly, AFM studies proved that phylogenetically-similar bacteria exhibit enormously different metabolic response towards *hydrophobic* polymeric surfaces.

Combinatorial surfaces for protein sensors and arrays.
Experiments regarding the adsorption of biomolecules on combinatorial surfaces focused on the actual physical attachment of biomolecules on several 'model' surfaces; or on combinatorially fabricated structures. A new process (patented) that uses the ablation of a very thin layer of metal on top of an underlying thermo-labile polymer substrate generates micro/nano-topographies with high reproducibility, comprising large variations of hydrophobicity. The adsorption of protein is amplified from 3- to 12-times for large and small proteins, respectively.

Impact. The AFM studies demonstrate the criticality of choosing polymeric surfaces for microfluidics applications (e.g. better polymeric surfaces for micro-PCR devices); and for a better selection of polymers for cell-based devices. Another possible impact is the rational design of bioactive, bacterial-specific surfaces (e.g. inherently antibacterial surfaces). The use of combinatorial surfaces can amplify the adsorption *and* the bioactivity of immobilized proteins for microarray sensor devices.

KEY PERFORMANCE INDICATORS

Several *key performance indicators* of the project are as follows:

- 13 journal papers published or in print; and 2 other submitted or in the process of submission;
- 19 conference full papers
- 1 database and 1 software package;
- 1 patent and associated commercialization effort;
- 2 explicit collaborative efforts, one within Bioflips program; one within Simbiosys program.

2.0 INTRODUCTION

In microfluidics systems, the flow of the fluids is well within the laminar regime. This would make the design trivial if not for a number of complications detailed below.

- The first fundamental complication arises from the fact that in the laminar regime almost all of the hydrodynamic resistance to flow is concentrated at the walls. This resistance is used to estimate the pumping power and resultant design. But what are the walls? In the conditions of biomolecules attaching -parasitically or indiscriminately- on the walls, the "rugosity" of the wall as well as its nature change, perhaps dramatically. Then the hydrodynamic resistance changes as well.

- Secondly, in the conditions of micron sized channels, corners etc. the non-specific attachment of the biomolecules on the walls importantly changes the dimensions of these features, therefore changing the hydrodynamic resistance to flow.

- Thirdly, although the flow is laminar, the fluids are unlikely to be Newtonian as the concentration of the biomolecules can be considerable. Moreover, the concentration of these biomolecules (and the associated change of the transport properties but also the reactivity of the sensing) are likely to change spatially (e.g. different concentration in corners than channels) subsequently changing the transport properties locally.

- Fourthly, during the functioning of the microfluidic device, numerous types of biomolecules -many without any sensing functionality- come in contact with the body of the device and nonspecifically attach on the walls or on sensing area.

Clearly, it is essential to either (i) eliminate the non-specific binding altogether; and/or (ii) to predict the effects of this attachment in an engineering, fully predictive manner. However, the elimination of non-specific binding, although proven feasible (e.g. by research performed by Whitesides' group, and Andrade's and co-workers) does not solve the situations were immobilization is needed, e.g. probe biomolecules on bio-sensing areas. Moreover, there are situations where the 'bio-objects, e.g. cells, are responsive to surfaces, or are too large and too complex for a universally repelling surface to be devised. For all of the above reasons, the engineering-style understanding, quantification and derivation of design-ready, engineering relationships is necessary.

The proposed project aimed at delivering scaling relationships regarding the non-specific attachment of biomolecules (and cells) on the walls of the microfluidic devices and the related impact on hydrodynamic design. The project used fundamental experiments, mostly focused on the use of Atomic Force Microscopy, and a combination of database building and engineering style regression to build-up the understanding regarding biomolecular/cell adsorption; and deliver relevant scaling relationships.

3.0 METHODS, ASSUMPTIONS, AND PROCEDURES

3.1 Database for biomolecular adsorption

A major part of the effort was focused on the building, upgrade and maintenance of a database comprising experimental data regarding biomolecules (in particular proteins) adsorption on different surfaces (in particular polymers). Apart from providing (in part) the experimental data needed for the construction of the model and/or for its validation, the database can serve in the short term as a reference for particular cases that have been already described in the literature. Additionally, the database (which is accessible at http://www.bionanoeng.com/bad) was conceived to be a forum of discussions and self-upgrade with data submitted to the database maintenance team.

The database was designed to have 3 elements:

- The adhesion database per se, BAD, which comprises experimental data regarding the actual concentration of the biomolecule on the surface and in solution, the polymer (or other surface), the solution data (pH, type of buffer), the experimental method used and the bibliographic data – where applicable. The database comprises a few hundred cases of protein adsorption on different materials. The database is organized along surface descriptors (surface tension and contact angle), environment descriptors (pH; ionic strength; and temperature), and protein descriptors.

- The biomolecule descriptors database, which comprises the parameters (extracted from the biomolecule structure) found to be relevant to adhesion. This part of the database was replaced later with the software that extracts molecular surface descriptors. The molecular descriptors regarding the protein (or any other biomolecule) are calculated with an in-house developed software package (freely available at the same site) that uses an upgrade of the Connolly's algorithm for the visualization of molecular surfaces.

- The polymer descriptors database. This database was not developed fully, as the relevant parameters can be derived from QSAR approaches (e.g. van Krevelen) for which commercially available software packages exist (e.g. PolySci). For the cases present in BAD, we estimated (where data was not available) the relevant parameters (i.e. surface tension/contact angle) and listed the values along with adsorption data.

3.2 Atomic Force Microscopy studies of biomolecular and cell attachment on polymers

A major part of the work was based on the use Scanning Probe Microscopy, or more narrowly, Atomic Force Microscopy (AFM).

3.2.1 Principles of AFM methodology

In the context of attachment of biomolecules to substrates, the following characteristics are relevant for the functionality of the substrate.

- Gross morphology - on a scale comparable to that arising from patterning
- Molecular scale morphology - relevant to that constraining conformational interactions
- Physical properties - hydrophobicity, patch charging, etc
- Chemical properties - covalent bonding sites.

The AFM system is uniquely capable of providing all-around characterization of polymer surfaces in air and aqueous environments on a single platform. It has exceptional lateral and depth spatial resolution when deployed as an imaging tool. In the force versus distance, F-d, mode it acts as a local probe of interaction with a force resolution of 1-10 pN and a dynamic range of μN. In the lateral force mode, LFM, it can discriminate, and map with high-resolution, regions with different surface chemistries. Additional chemical information can be obtained in the F-d mode by functionalizing the probe tip. A schematic of a generic AFM system is shown in Figure 1.

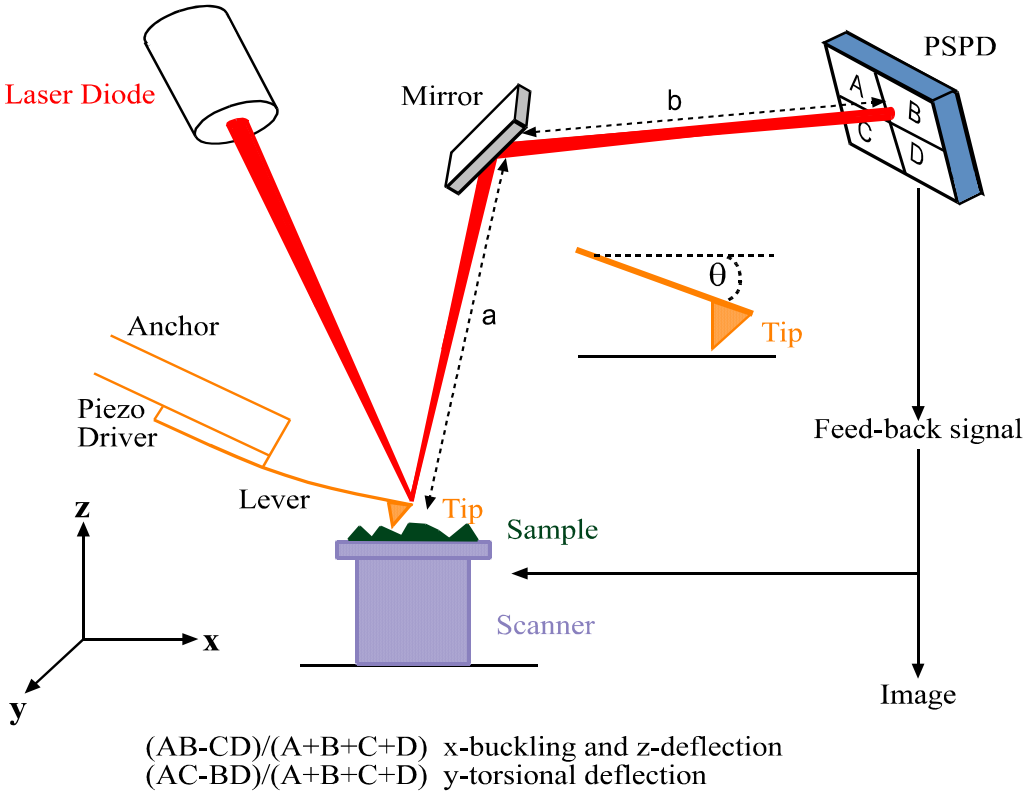

Figure 1. Working principle of Atomic Force Microscopy.

As an imaging tool the AFM offers both qualitative and quantitative information about surface topography. Likewise, work by the research group and by others has shown that quantitative information is also obtainable in the LFM mode, and that it is possible to define a 'best practice'.

In the case of F-d analysis, it has proven difficult to generate quantitative and reproducible results on a routine basis, although many informative and elegant experiments have been performed. This mode is potentially an extremely rich source of information. A generic F-d curve is shown in Figure 2 for a 'hard' tip making contact with a 'hard' surface. In this context, 'hard' refers to an assumption that the two bodies in contact are incompressible; equivalently it can be said that the effective spring constant of interaction is much greater than the spring constant of the force-sensing/imposing lever. The part of the curve where the tip senses a strong short-range interaction is due to adhesion, which normally arises from a meniscus force due to adsorbed moisture.

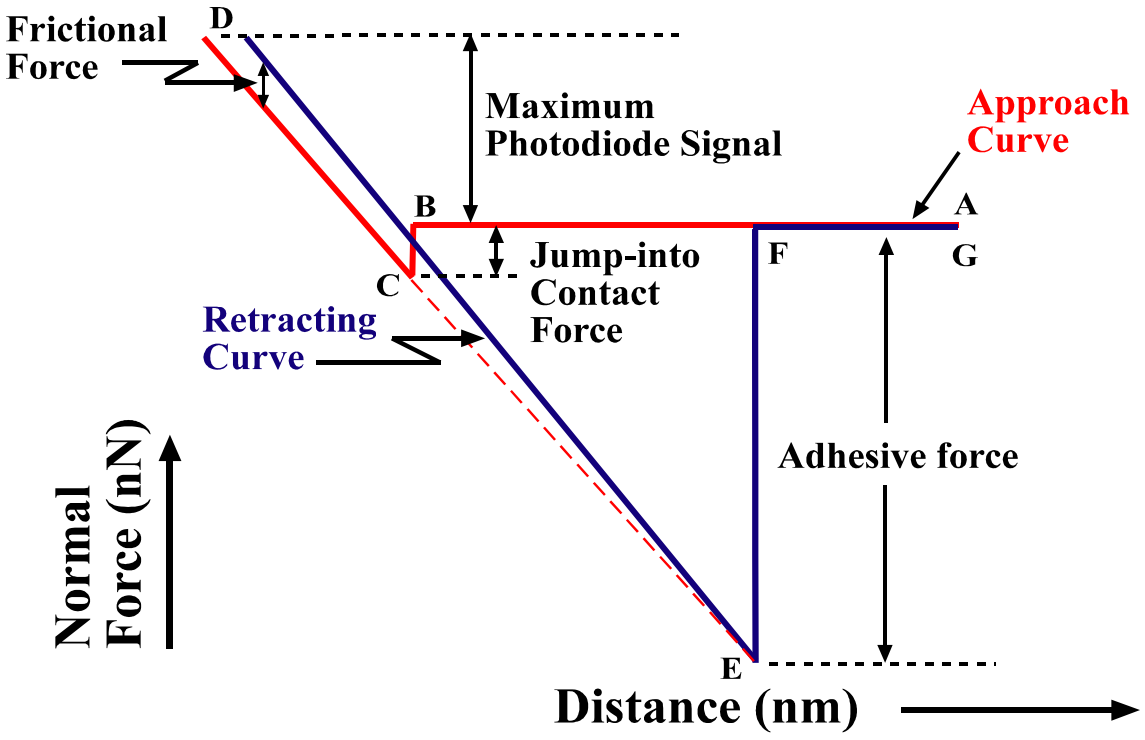

Figure 2. Principle of the measurement of attachment and repelling forces with AFM.

It may be difficult to extract quantitative data from an F-d curve for the following reasons, most of which apply to analysis of polymer surfaces.

- Either or both of the surfaces in contact may be compressible; thus the tip-to-surface contact area will depend on the net effect of attractive and repulsive forces.

- The surface topography of the specimen may differ from one region to another, or from one specimen to another; the contact area will therefore be different.
- The shape of the tip, in the nanoscopic or mesoscopic regimes, may change from one tip to another, or it may change during the course of an experiment; the tip may wear or it may pick up debris from the surface or from the ambient.
- The surface chemistry of the tip may change during an experiment; e.g., material may be transferred from the surface, or from the ambient, to the tip.

In practice it may be difficult, usually impossible, to eliminate all of these sources of uncertainty. The following strategies have been tailored and validated for dealing with the particular problems and requirements presented by bioactive polymer surfaces.

- A 'standard' configuration is being developed that will produce the most reliable and detailed characterization of polymer surfaces.
- A 'standard' protocol is being developed in order to deploy most effectively the standard configuration.
- Two types of standard specimens have been adopted. Industry standard Si wafers can readily be obtained with RMS roughness of < 1nm, and with known surface chemistry (arising from the presence of a thin native oxide). As well, there are well-established methods for cleaning such surfaces. The second surface consists of gold evaporated onto a Si substrate. Again, the outcome is known and has reproducible surface topography, surface chemistry and physical properties. Thus, all subsequent data from F-d analysis can be referenced back to data obtained from one or both of the standard surfaces.
- Adoption of standard tip topographies and properties relevant to the conditions of the specimens being investigated. A typical as-received micro-fabricated Si or Si_3N_4 tip is coated with a native oxide and will have a nominal radius of curvature at the apex of ca. 50 nm. The performance of such a tip may be 'normalized' through analysis of a standard surface. Alternatively, a bead of known radius of curvature and known surface chemistry may be attached to the lever. Again, the performance may be 'normalized' through analysis of a standard surface. It is envisaged that experiments will be designed in such a way that the integrity of the tip can be verified at any stage during an analysis run by returning to the standard surface.

3.2.2 Attachment of beads

One of the main novelties of our approach consisted in the measurement of the average forces between 'model' surfaces and 'model' proteins. Usually, the measurement of forces between individual amino acids and surface will inherently measure one side of the interaction, depending on what side of the amino acid is attached on the AFM tip, with little relevance to the actual molecular surface on the protein. Therefore, our approach consisted of attaching beads on AFM cantilevers and functionalization of these beads with model proteins (i.e. mono-AA proteins, e.g. poly-lysine; poly glutamic acid etc.); the measurement of the forces between an 'average' protein surface and a surface.

Beads of any diameter in the range 5-100 μm (with or without additional surface functionalization) can be reliably attached to standard AFM levers. The procedures take advantage of the capabilities inherent in the AFM instrument for locating and attaching the bead at the end of the lever, so that the mechanical characteristics of the probe are unaffected by the procedure. See optical image in Figure 3 for an example of the outcome of attaching a 70 μm diameter bead (BioRad S-X styrene divinylbenzene for exclusion chromatographic applications) to an AFM cantilever.

Figure 3. Probing bead attached on an AFM cantilever.

3.2.3 Structure of biomolecular and cellular thin films on polymeric surfaces

AFM characterization was performed using a TopoMetrix Explorer (ThermoMicroscope) in both non-contact and contact modes. Several scanners were used and the field-of-view ranged from 100x100 μm^2 down to 2x2 μm^2. Pyramidal-tipped, silicon nitride cantilevers with a spring constant of 0.032 N/m were used in the contact mode, whereas silicon cantilevers with a spring constant of 42 N/m and resonant frequency of 320 KHz were used in the non-contact mode. As the tip is scanned across the surface in the contact mode, the frictional force acting on the tip manifests itself through a torsional deformation of the lever, which is sensed by the difference in the Left-Right signal on the quadrant detector. It is important to note that both friction and topography contribute to the lateral forces. The contrast due to friction is inversed upon reversal of scan directions, whereas the topographical contrast is independent of the scan direction. The contrast reversal in the lateral force image has been used as an important indicator for deciding whether the contrast is caused by topography or friction. In principle, the topographical contribution to the lateral force image may be removed by subtracting images recorded in the forward and reverse directions; and the difference is the frictional force acting between the tip and the sample.

In the present study, the lateral force imaging was performed simultaneously with topographical imaging in both forward and reverse scan directions. In the interest of brevity and conciseness, only subtracted lateral force images of features, which have contrast reversal upon reversal of scan direction, are presented. Image subtraction and root-mean-square (RMS) surface roughness calculations were carried out using the Explorer software.

Elemental analyses of plasma-treated polymeric surfaces were carried out on a Kratos Ultra Imaging X-Ray Photoelectron Spectrometer (XPS), using monochromatized Al Kα (photon energy = 1486.6eV) radiation at a source power of 150 W. The analysis areas were nominally ~ 700x300μm^2. Wide scan and region scan spectra were acquired using 160eV and 20eV pass energies, respectively. Electron binding energies were calibrated against the C1s emission at 284.6eV.

3.3 Adsorption of biomolecules on combinatorial surfaces

The first line of (reduced number of) experiments aimed to study the actual physical attachment of biomolecules on several 'model' surfaces; or on combinatorially fabricated structures. Several photosensitive polymers have been investigated, both photo-acid and photo-base-generated polymers. The chemical schemes for the respective photopolymers, i.e. Poly(tert-butyl methacrylate); Diazo-naphto-quinone/novolak; and O-acryloyl acetophenone oxime (AAPO) polymer are presented in Figures 4-6.

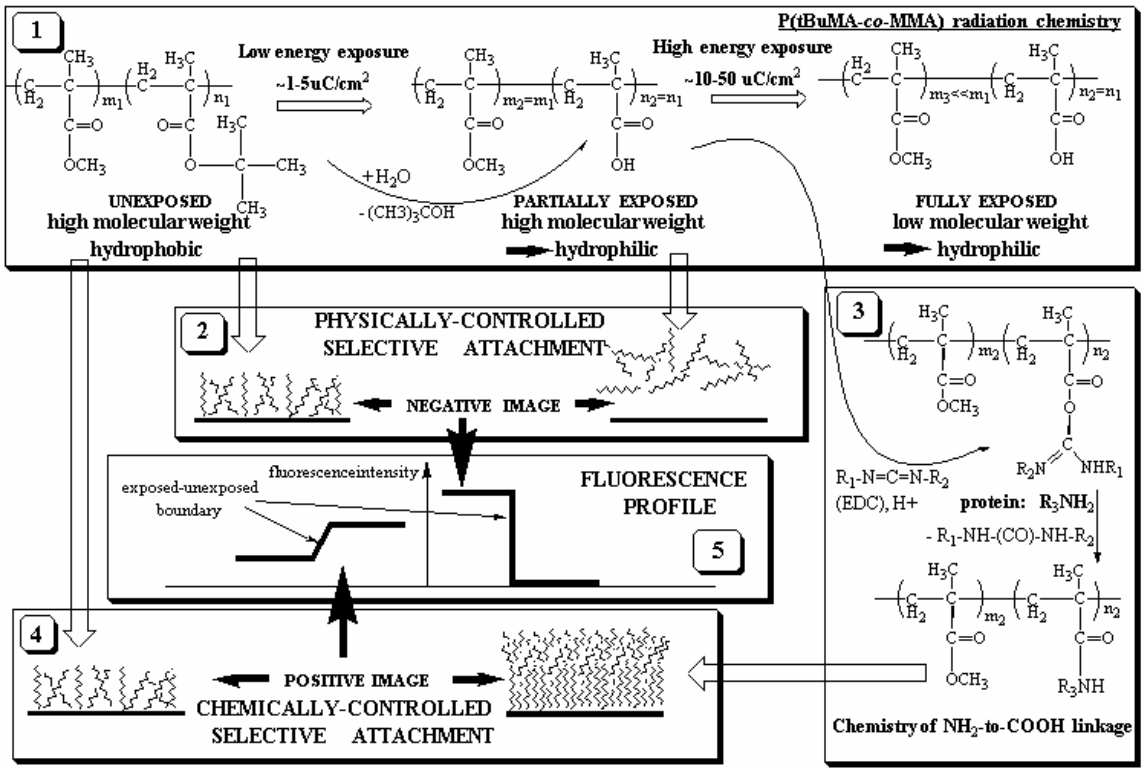

Figure 4. Radiation chemistry and associated mechanisms for spatially selective protein immobilization for P(tBuMA).

Another line of experimentation used the combinatorial surfaces generated using a process (now patented) that relies on the ablation of a very thin layer of metal (~50nm or less) to process thermally and in-situ the top surface of an underlying thermo-labile polymer substrate. This process generates micro/nano-topographies with high

reproducibility, comprising large variations of hydrophobicity, from highly hydrophobic (concentrated in the middle of the ablated area) to hydrophilic (at the edges) micro/nano-surfaces. An outline of the process is presented in Figure 7.

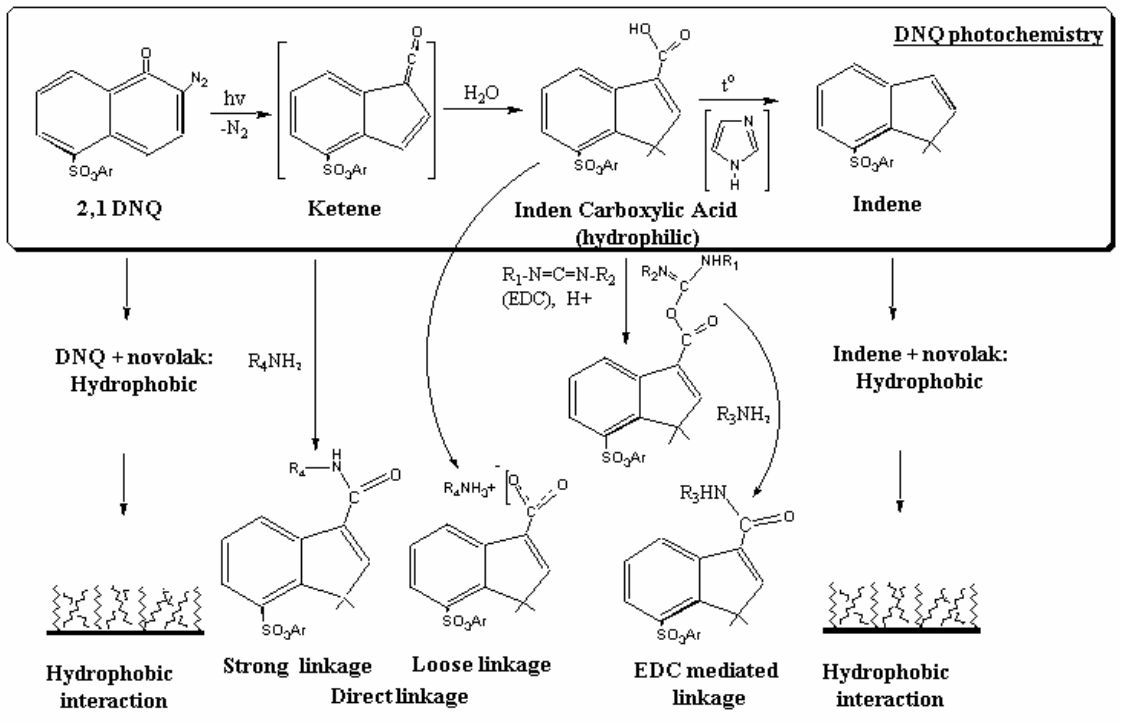

Figure 5. Radiation chemistry and associated mechanisms for spatially selective protein immobilization for DNQ/novolak system.

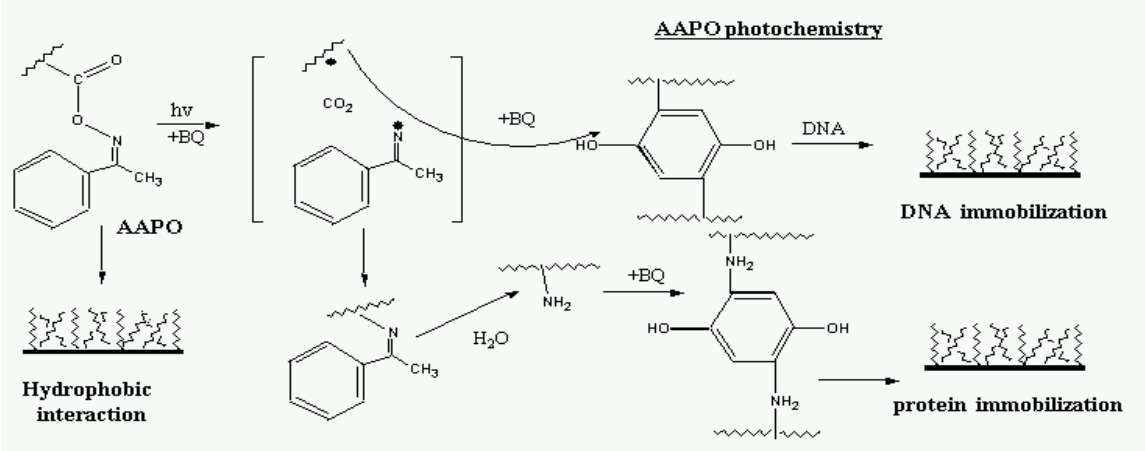

Figure 6. Radiation chemistry and associated mechanisms for spatially selective protein immobilization for AAPO system.

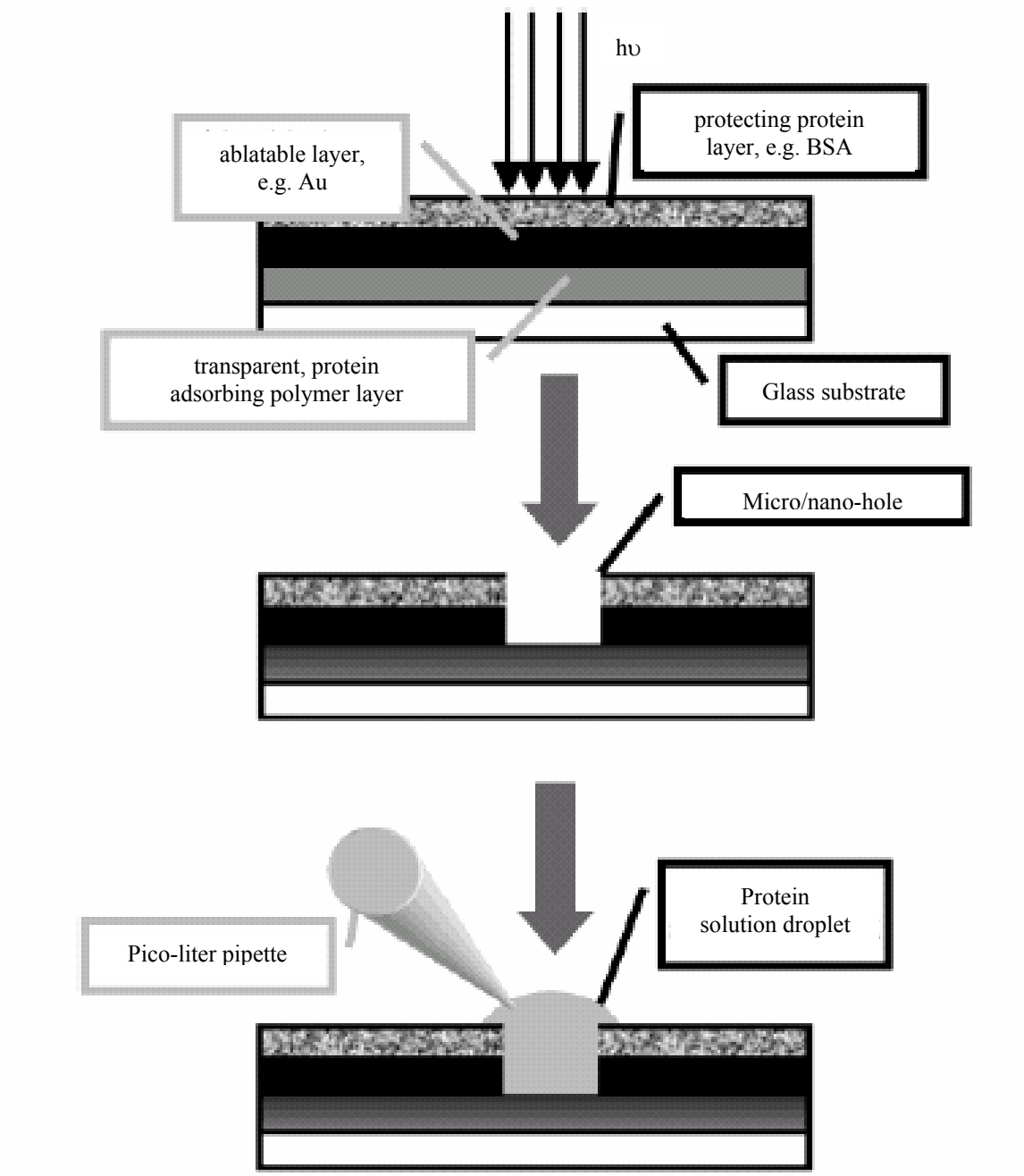

Figure 7. Process for obtaining combinatorial surfaces on the top of polymeric surfaces.

3.4 Scaling relationships regarding biomolecule adsorption on polymeric surfaces

The scaling relationships have been built comparing potentially relevant descriptors, i.e. biomolecular descriptors; surface descriptors; and environment descriptors with adsorption data present in the database. Apart from helping to build the adhesion model, an additional benefit of the biomolecule descriptors database is that it allows the

establishment of general relationships *between* these descriptors. These relationships are important for the many cases where structural data regarding biomolecules is not available. For instance, in many cases only the molecular weight of the biomolecule is available and perhaps the isoelectric point. Very general approximate relationships for biomolecular adsorption can be used to assess the impact of geometry change, especially for the devices that use very narrow (hundreds of nm to few microns) structures.

The connectivity between molecular descriptors, or lack of these, is succinctly presented in Figure 8. First, several descriptors that can be inferred from the crystallographic structure of the biomolecules can be correlated with "simpler" descriptors, e.g. molecular weight (Mw). Second, other descriptors are actually almost constant, and therefore an average value could be used in the prediction of adhesion. Third, there are other descriptors which are truly unrelated to lower level descriptors, and therefore they have to be estimated in order to have a proper approximation of the adhesion.

The scaling relationship predicting the ablation rates relies on laser descriptors (fluence and wavelength) and the descriptors of the ablated material (density, Tg and optical absorption).

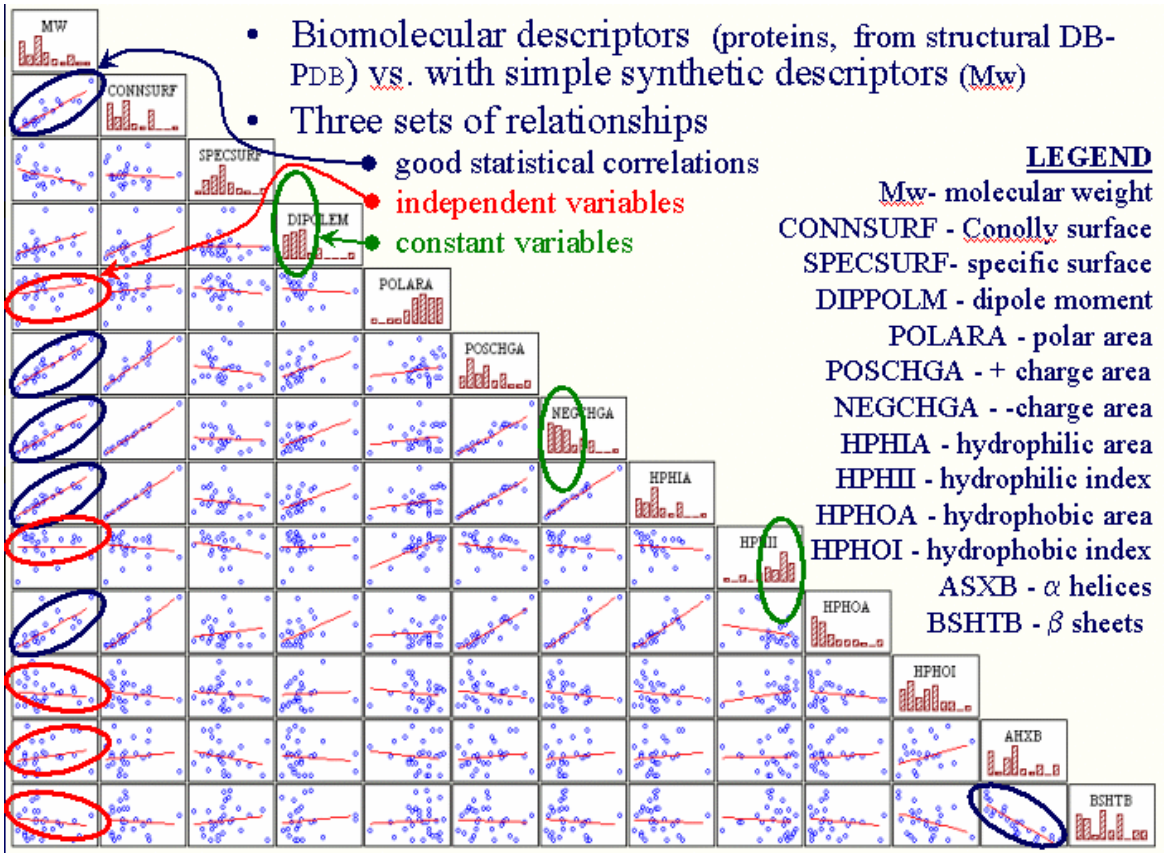

Figure 8. Interconnectivity between biomolecular adsorption-relevant descriptors.

4.0 RESULTS AND DISCUSSION

4.1 Database for biomolecular adsorption

The database is organized along surface descriptors (surface tension and contact angle); environment descriptors (pH; ionic strength; and temperature); and protein descriptors. The molecular descriptors regarding the protein (or any other biomolecule) are calculated with an in-house developed software package (freely available at the same site) that uses an upgrade of the Connolly's algorithm for the visualization of molecular surfaces.

The site, comprising the database and a downloadable version of the software, has been used by many thousands of researchers and visited a few hundred times per week over the period of the last 2 years. The database will be maintained in the future with funds from the proposing University.

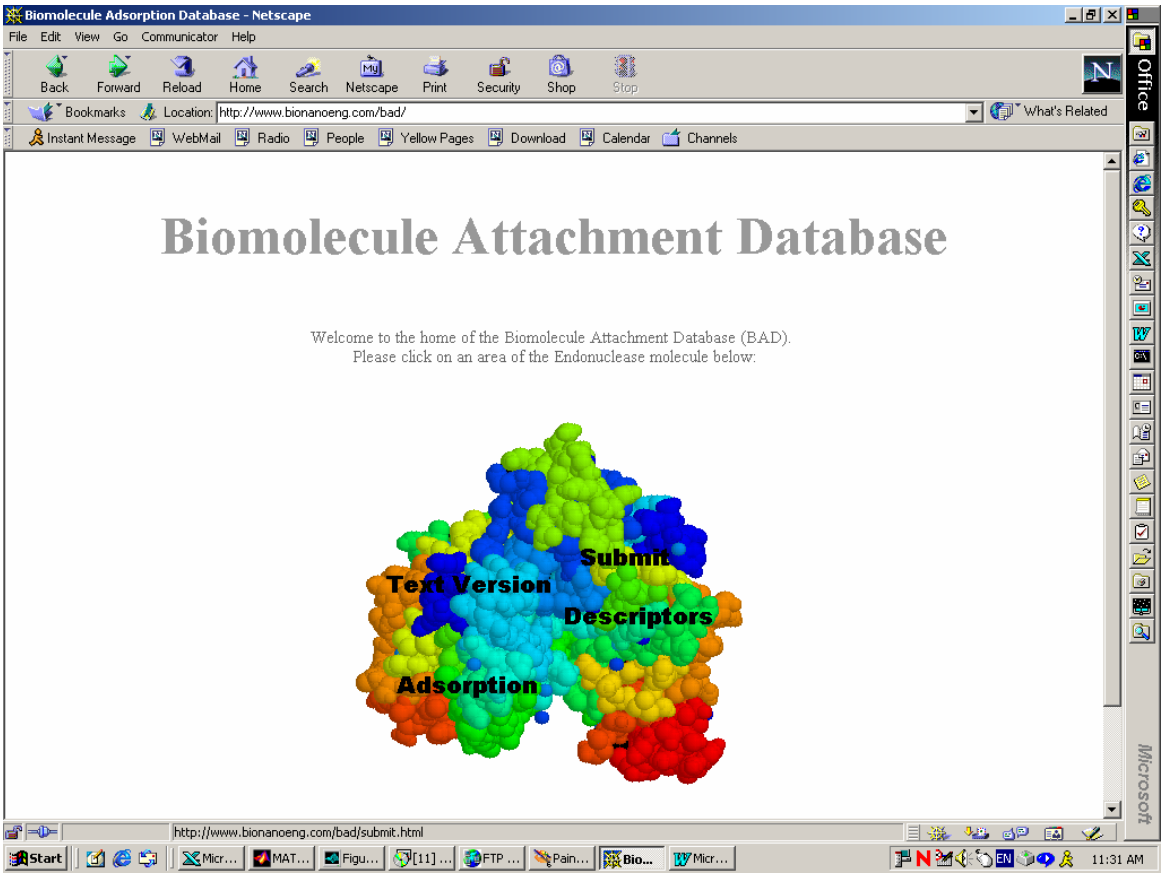

Figure 9. Screen-out of the entry to the Biomolecule Attachment Database (BAD).

The database, which also has a text-only, downloadable version, allows searches for types of surfaces and protein type. Examples of screens for database searches are presented in Figure 10.

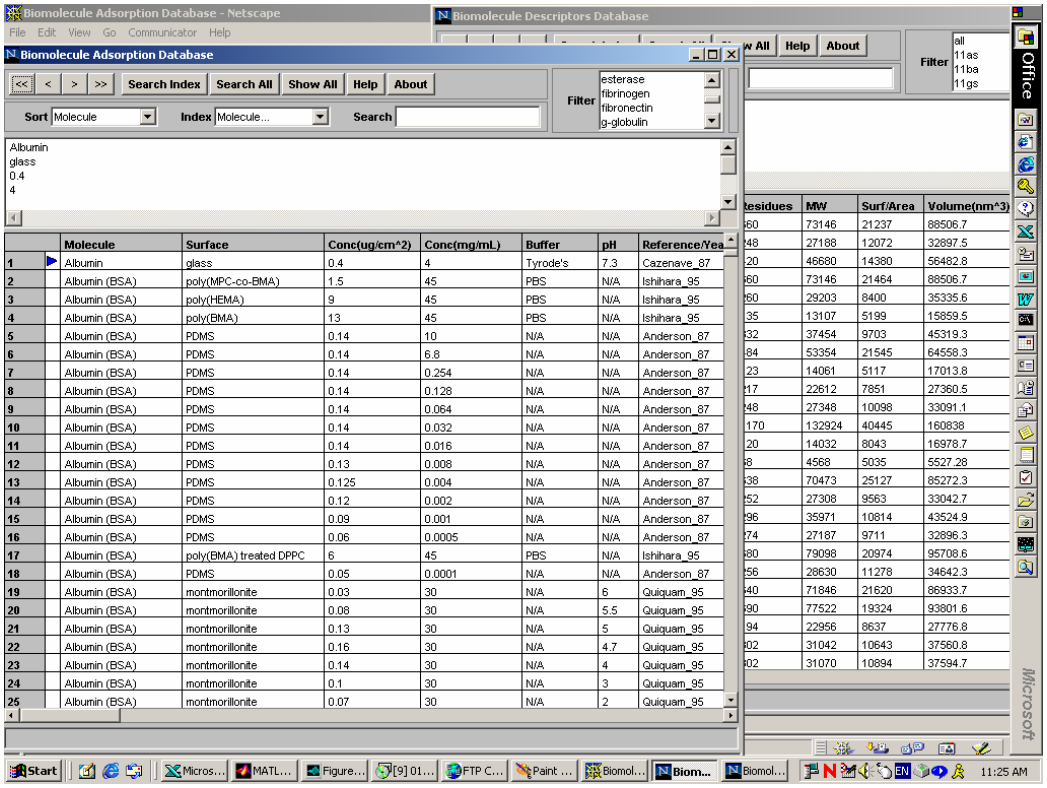

Figure 10. Screen-out of the search pages of the Biomolecule Attachment Database.

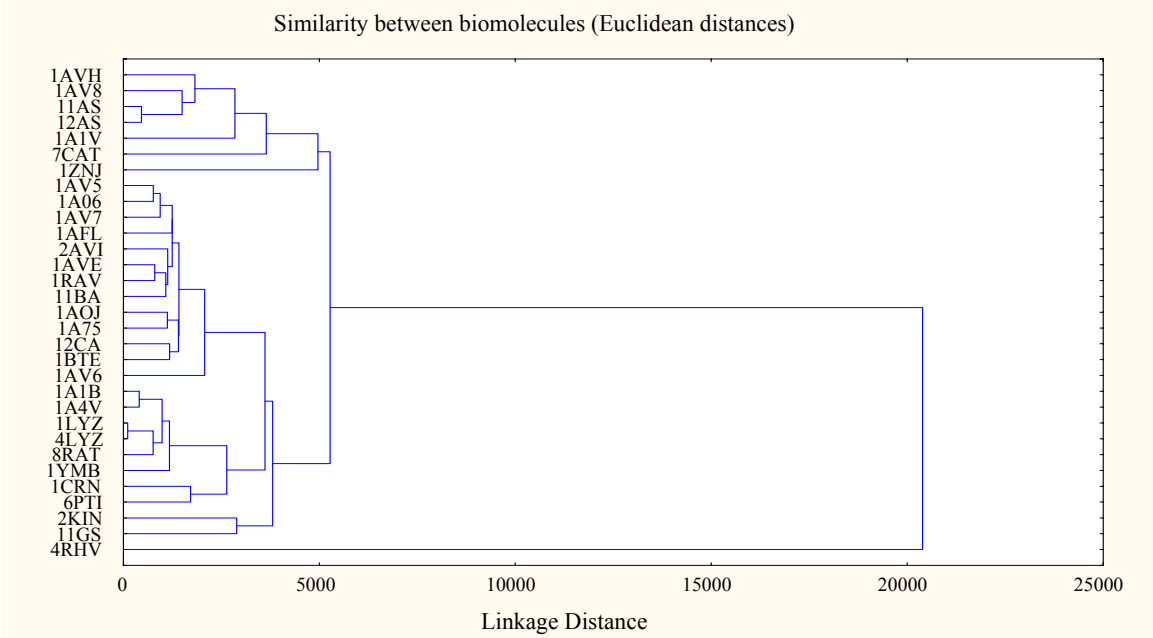

Figure 11. Clustering of the proteins present in the database.

In many instances an explicit relationship is not possible to find, for instance because there is some uncertainty regarding the molecular structure of the adsorbed protein or because the PDB structure is not available. For these situations, and if some information regarding the similarity (e.g. pI, molecular weight) between the unknown protein and other proteins exists, then an approximation can be made through the comparison of adsorption data with similar proteins. Figure 11 presents three clusters of the proteins present in BAD, clustered along molecular descriptors.

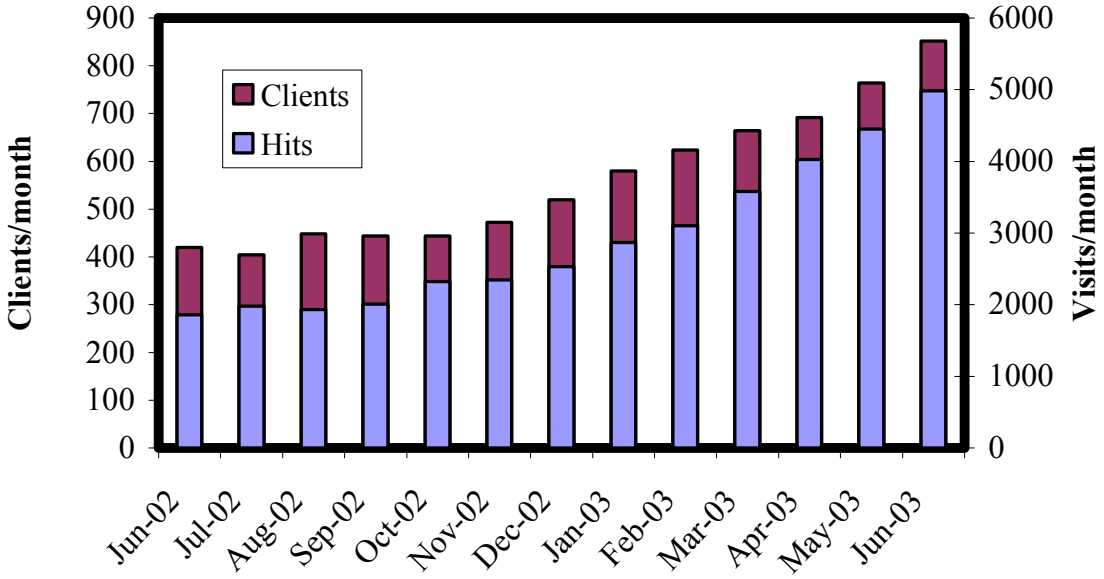

Figure 12. Frequency of visits/hits/downloads from the BAD site.

4.2 Atomic Force Microscopy of biomolecular and cellular attachment on polymers

4.2.1 Fundamental forces between model proteins and model surfaces

Biomolecules in a confined solution environment may be subject to electrostatic forces with a range up to 100 nm, while van der Waals interaction will account for shorter-range forces. The response of two model poly(amino acids) - poly-L-lysine and poly-L-glutamic acid - has been investigated for a silica/Si-oxide surface at pH 6. The model amino acids were adsorbed, or covalently coupled, to colloidal probes consisting of a microsphere attached to a force-sensing lever. The methodology was based on sensing interaction between the probe and a flat surface by performing F-d analysis with a scanning force microscope. The results were analyzed within the framework of the conventional DLVO theory. The outcomes illustrate both repulsive and attractive long-range interactions that will hinder, or promote, colloidal biospecies in solution entering the region of attractive short-range interactions at the physical interface. Large 'snap-on' distances were observed for some systems and have been ascribed to compression of the 'soft' functionalized layers. Those observations and measurements of adhesion provided insight into conformation of the adsorbed species and strength of attachment. The results

have implications for the efficacy of methods and devices that seek to exploit the properties of micro/nano-fluidic systems. Further studies comprising more 'model' proteins would allow the building of a 'look-up' table for the force of attraction/repulsion as a function of respective amino-acid. This look-up table can then be indexed, in connection with the molecular descriptors software, on the surface of any protein with known structure; and then integrated to give an overall attraction/repulsion effect.

The 'snap-on' distances and the correlation with the respective measured forces of attraction for model surfaces and model adsorbents, including model proteins, are presented in Figure 13.

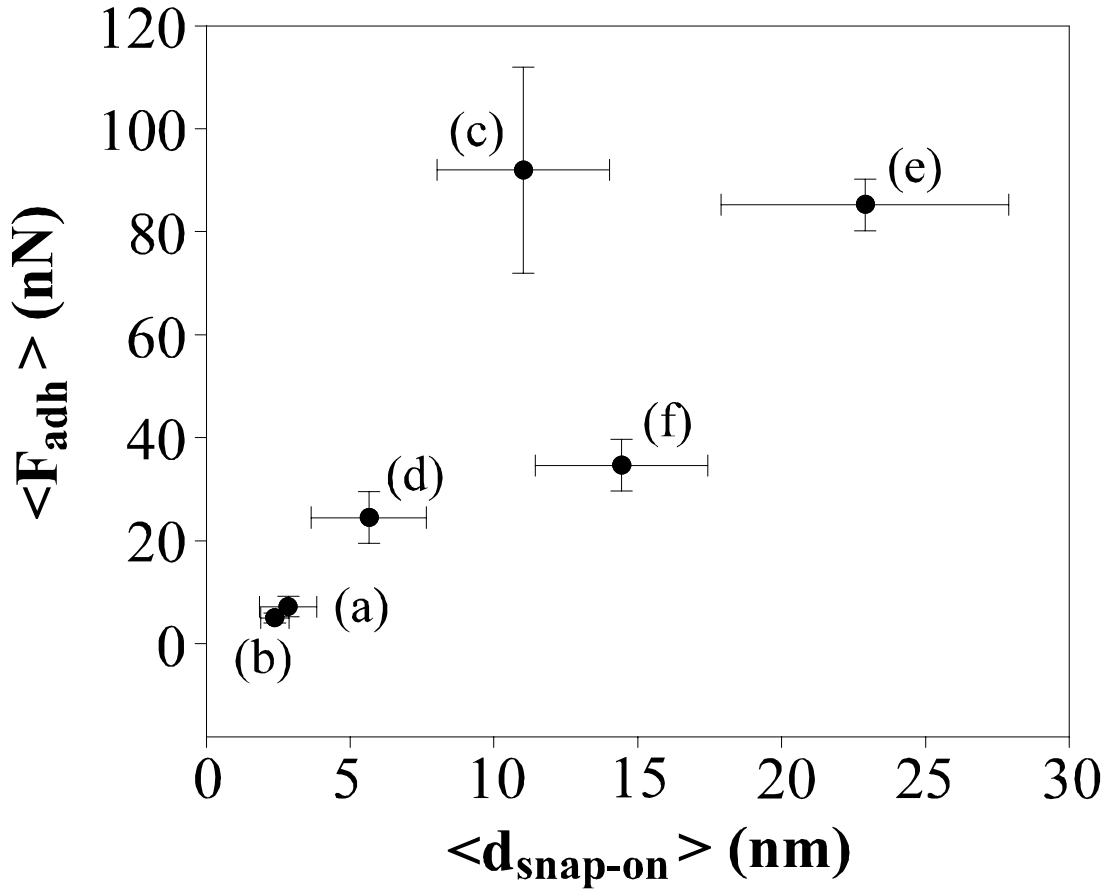

Figure 13. Average snap-on distance versus average adhesion for the combinations of probe and surface investigated in the present study. The labels refer to: (a) silica vs. SiO_2; (b) silica vs. Y_2O_3; (c) silica/COOH vs. SiO_2; (d) silica/lysine vs. SiO_2; (e) silica/COOH/lysine vs. SiO_2; (f) polystyrene/NH_2/glutamic vs. SiO_2/lysine.

The system consists of a dielectric sphere interacting with a planar surface of a semi-infinite dielectric solid. Both objects have interfaces with, and are submerged in, an aqueous medium. Bound charges will, in general, be present at the interface between the solid and liquid. Boundary conditions require that the effective potential decays

exponentially away from the surface at a rate defined by the Debye length, κ^{-1}. At separations > 10 nm, an electrostatic interaction arising from the overlap of the double layers will generally dominate over other interactions. At smaller separations the attractive van der Waals interaction becomes increasingly dominant. In the context of an SFM-based experiment, the sphere will be attached to the end of a force-sensing/imposing lever; the force-response of the lever is described by $\Delta F_L = k_N \Delta z_L$, where k_N is the spring constant corresponding to normal deflection, Δz_L, of the lever. At a separation between sphere and plane of d, the static force imposed by the lever is balanced by repulsive and attractive components acting on the sphere due to electrostatic, F_E, and van der Waals, F_{vdW}, interactions.

The two contributions to the force are conventionally described by the DLVO theory. The double layer interaction between a sphere and a flat surface is given by

$$F_E(d) = -\left[\frac{4\pi R\sigma_1\sigma_2}{\varepsilon\varepsilon_0\kappa}\right]\exp(-\kappa d) \qquad (1)$$

where R is the radius of the sphere, σ_1 and σ_2 are the respective surface charge densities, ε is the relative permittivity of the aqueous medium, and ε_0 is the permittivity of free space. The Debye length will depend on the concentration and valence of species in the bulk solution, in accordance with

$$\kappa^{-1} = \sqrt{\frac{\varepsilon\varepsilon_0\, kT}{e^2\sum n_i^{\infty} Z_i^2}} \qquad (2)$$

where k is the Boltzmann constant, n_i^{∞} is the concentration of i-type ions in bulk solution and Z_i is the ionic valence. Van der Waals force for the same geometries is given by

$$F_{vdW}(d) = -\frac{HR}{6d^2} \qquad (3)$$

with H being the Hamaker constant.

The constants in the relationships (1-3) for the 'model' systems are presented in Table 1.

Table 1. System characteristics inferred from application of DLVO analysis.

System	σ_1(C/m^2)	σ_2(C/m^2)	κ^{-1}(nm)	H_{eff}(10^{-20} J)
Silica vs SiO_2	-1.8×10^{-3}	-1.8×10^{-3}	27	2.0±0.5
Silica/COOH vs SiO_2	-3.5×10^{-3}	-1.8×10^{-3}	25	na
Silica/lys vs SiO_2	4.7×10^{-3}	-1.8×10^{-3}	11	2±1
Silica/COOH/lys vs SiO_2	1.9×10^{-3}	-1.8×10^{-3}	30	2.4±1.5
Polystyrene/NH_2/glut vs SiO_2	-2×10^{-4}(?)	-1.8×10^{-3}	60-80(?)	na
Polystyrene/NH_2/glut vs SiO_2/lys	-4.4×10^{-4}	4.7×10^{-3}	21	na

The study shows that colloidal probe analysis implemented on an SFM platform constitutes a convenient and informative method of investigating intermediate range interaction arising from double layer effects between biospecies in solution and bioactive surfaces and interfaces. It will also provide insight into adhesion and conformation of adsorbed species.

The outcomes have important implications for devices and processes that are affected by static and dynamic properties of micro/nano-fluidic confinement of bio-colloids. The impact may constitute a threat, but may also provide opportunities. For instance, one may envisage a design that exploits double layer effects for pre-treatment or conditioning of a biofluid, or indeed a mechanism whereby filtering can be achieved.

4.2.2 Structure of DNA, protein films and cells on polymer surfaces

4.2.2.1 Structure of DNA on polymeric surfaces

We studied the immobilization and hybridization of amino-terminated oligonucleotide strands to cyclo-olefin-copolymer (COC) and polycarbonate (PC) surfaces, in the view of the potential applications in integrated microfluidics devices containing micro-PCR reactors and low cost hybridization arrays. The oligonucleotides were covalently bound to the plasma-treated COC and PC surfaces via an N-hydroxysuccinimide (NHS) intermediate. Analysis by AFM showed that the oligonucleotides were present on the surfaces as aggregates, and that the size, both vertically and laterally, of these aggregates on the COC surface was larger as compared to those on the PC surface. The immobilization density of the former was also higher (15.8×10^{12} molecules/cm^2) as compared to the latter (3.3×10^{12} molecules/cm^2). The higher density occurring on the COC surface is attributed to more effective NHS-functionalization and greater surface roughness. Subsequent hybridization doubled the height of the aggregates, while the lateral dimensions remained essentially unchanged. The preservation of the lateral dimensions is explained in terms of highly selective immobilization of the complementary DNA on the previously immobilized ssDNA; and the increase in height is explained in terms of the organization of the long probe strands used on the surface as flexible, coil-like polymer chains, which allow the complementary oligonucleotides to bind and increase the height of the aggregates due to larger rigidity of the double-stranded DNA.

The most interesting result regarding the structure of DNA films has been revealed by LFA which showed that while the ssDNA layers (in lumps) are more hydrophilic than the underneath surface (background), the hybridization reversed the “hydrophilicity/ phobicity image”, with more hydrophobic dsDNA aggregates than the background. These results are presented synthetically in Figure 14. Several mechanisms have been proposed: (i) change of the surface chemistry, and subsequently the hydrophobicity, following the treatment with hybridization buffer (containing e.g. surfactants); (ii) molecular ‘reconstructuring’ of the ssDNA and dsDNA layers, respectively on the surface, with different parts of the DNA strand being presented upwards to the AFM tip;

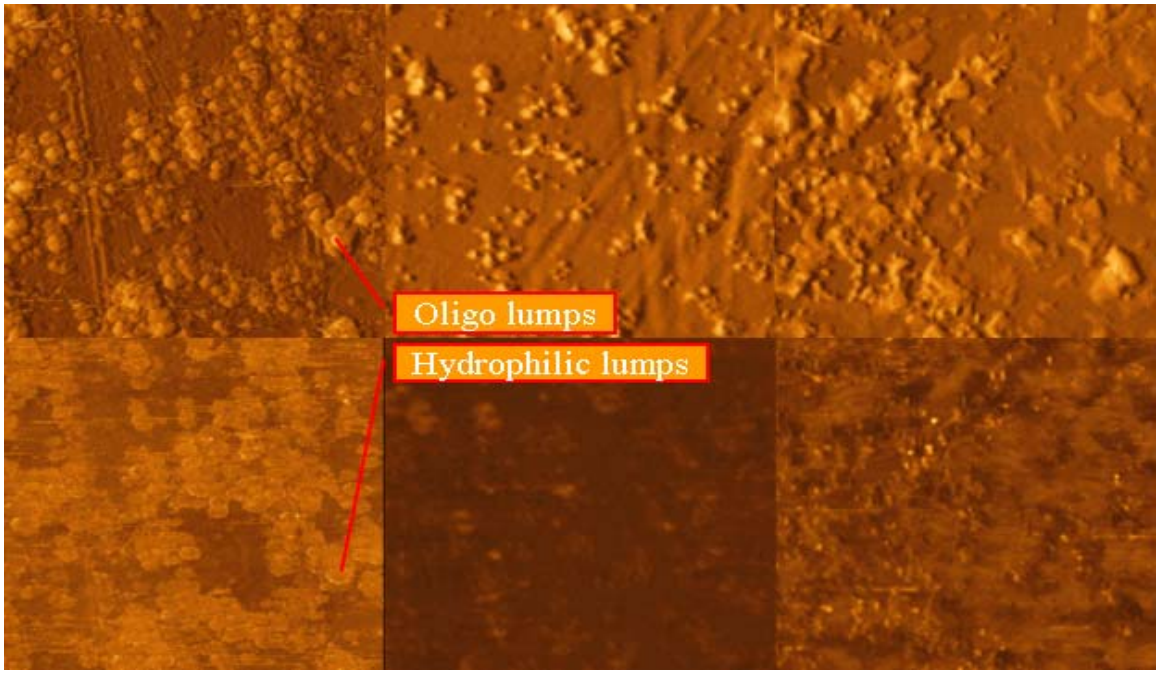

Figure 14. Topography (top) and lateral force (bottom) of the DNA layer after covalent binding on PCOC (left), PC (middle) and PSMA (right) surface.

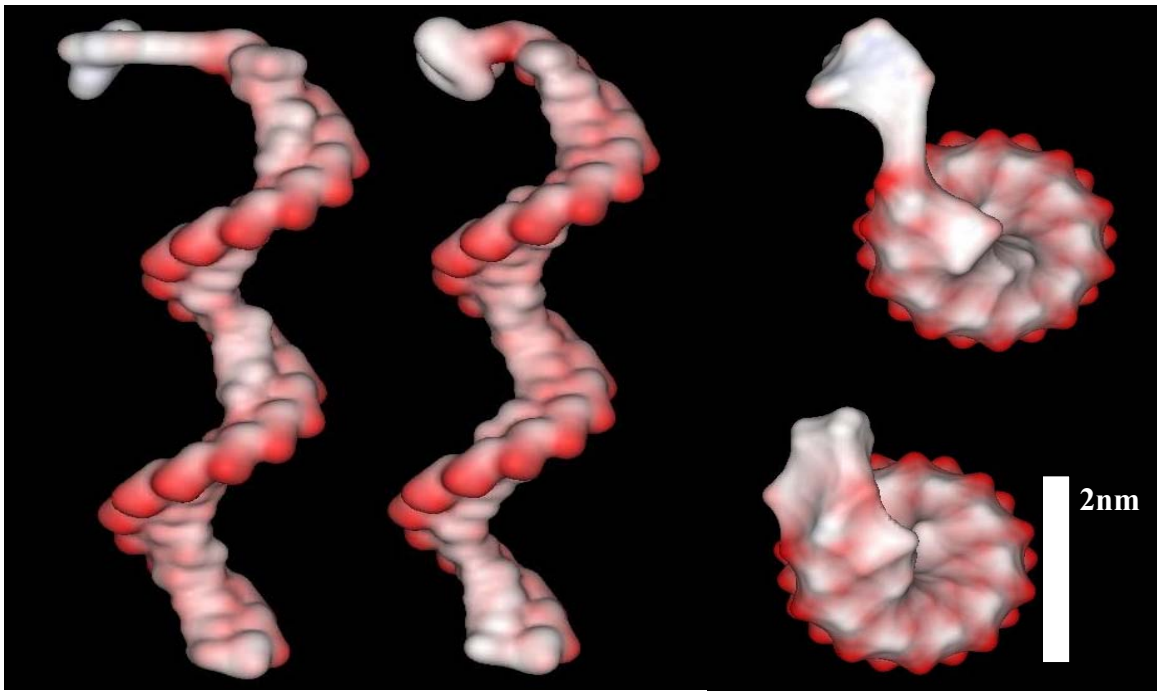

Figure 15. Electrostatic potential map of the Cy5-tagged oligonucleotide (far left; and top right) and complementary FAM-tagged oligonucleotide (middle and bottom right) as seen from the side and probed with a resolution of 1.4.Å (left structures); and from the top. The white areas are hydrophobic and red areas are hydrophilic (negatively charged).

and (iii) molecular 'reconstructuring' of the fluorescence tags (with different hydrophobicities) in relation to the DNA strand, prior and after hybridization.

The detection of the hydrophobicity of 'hydrophobic markers' (fluorescent tags) by a scanning probe is effectively a measure of the flexibility of the oligonucleotide layer and -consequently- the degree of hybridization (Figure 15).

Whatever the mechanism, this effect can be used in principle for the detection of nano-dots of DNA in advanced microarray devices (e.g. nanoarrays). The relatively high immobilization efficiency coupled with the stable thermo-mechanical properties make these polymers promising candidates for DNA-DNA hybridization assays integrated with PCR applications (e.g. Motorola microfluidics).

4.2.2.2 Structure of proteins on polymeric surfaces

The structure of the protein layers on surfaces is much more difficult to analyze with the AFM because the structure of the proteins (as opposed to DNA molecules) is very different in dry and wet/under solution state, with the latter being much more relevant but also much more difficult to analyze. Therefore, AFM can give only an indicative image of the structure of protein layers, and only for rigid proteins. Figure 16 presents a comparison of a protein layer immobilized on a hydrophobic surface.

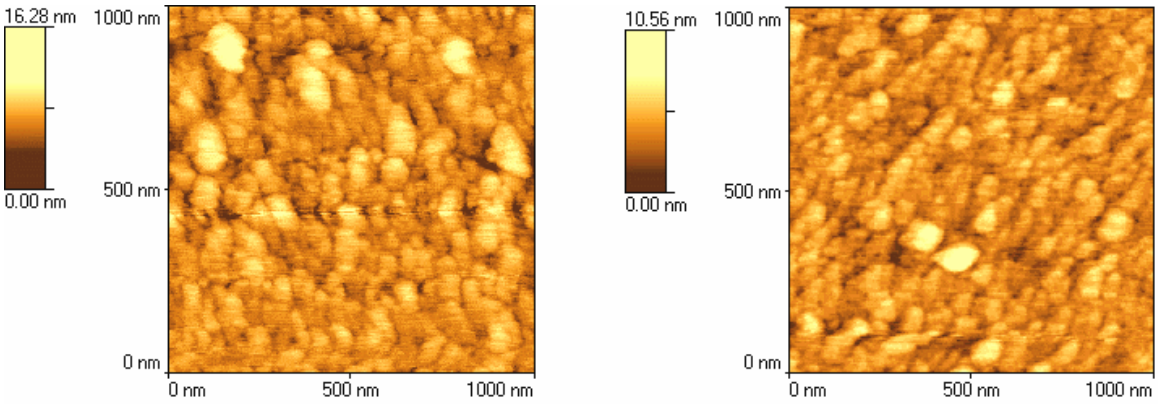

Figure 16. Protein (HeavyMeroMyosin, HMM) layer topography on Poly(tert butyl methacrylate) surface, immobilized by covalent binding (left) and adsorption (right).

4.2.2.3 Bacterial cells on polymeric surfaces

Another line of AFM experiments focused on the structure and metabolic response of the bacterial cells on several polymeric surfaces. It has been found that philogenetically close-related bacterial species have quasi-identical response towards polymeric hydrophilic surfaces (repelled); but exhibit enormously different metabolic response towards hydrophobic surfaces (i.e. repelled; overproduction of extra-cellular polymers; and switch to a vegetative form). These results are useful to a better selection of polymers for microfluidics applications (e.g. better polymeric surfaces for micro-PCR devices); and

for a better selection of polymers for cell-based devices (e.g. materials that have the potential to lyse the cells). A summary of the most important results on the structure and metabolic response of bacteria on surfaces is presented in Figure 17.

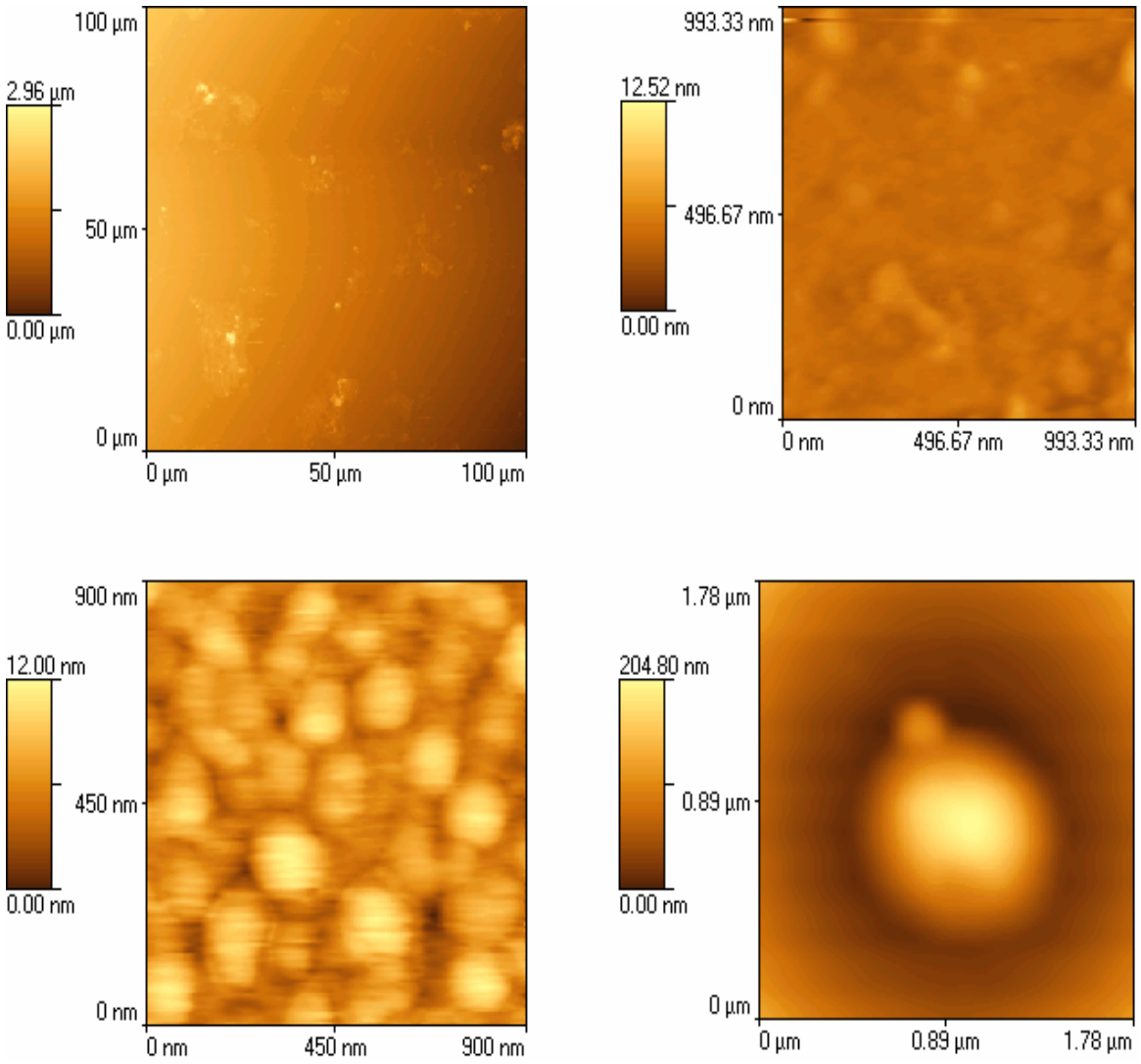

Figure 17. Top: S. pontiacus and S. brevis failed to attach to the hydrophobic PtBMA. The extra cellular matrix (ECM) is not present at all - cells cannot attach on very hydrophobic surfaces. Left-bottom: Under the same hydrophobic stress S. gluttiformis creates ECM. Right-bottom: Under the same stress, the vegetative cells of S. mediterraneus underwent a rare morphological conversion into coccoid forms during the attachment over an incubation period of 24-72 h.

4.3 Adsorption of biomolecules on combinatorial surfaces

The first line of (reduced number of) experiments aimed to study the actual physical attachment of biomolecules on several 'model' surfaces; or on combinatorially fabricated structures. Several photosensitive polymers have been investigated, and their photo-

generated hydrophobicity change has been measured by AFM/LFA. Figure 18 presents some AFM data for Poly(tert-butyl methacrylate) and photosensitive polyimides.

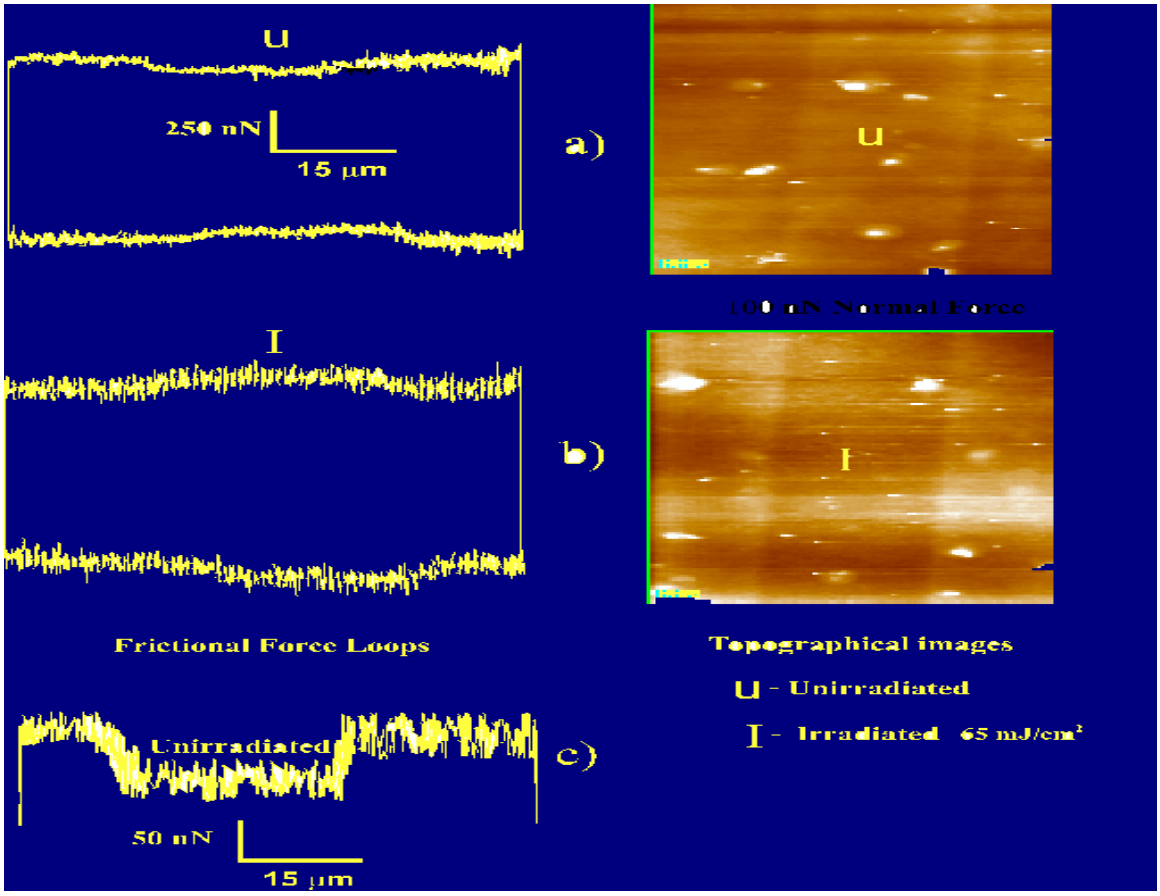

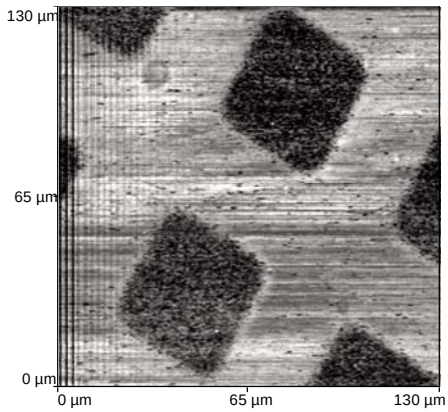

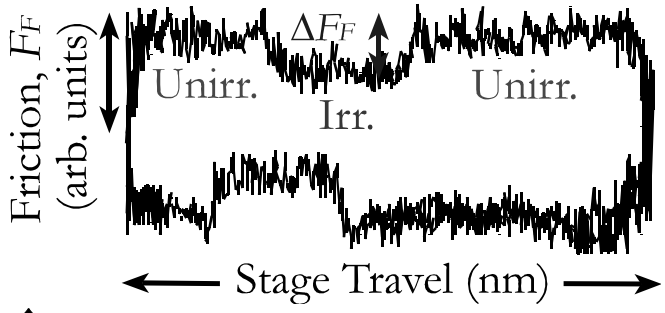

←↑ Lateral (friction) force image of UV-patterned polyimide revealing chemical contrast. Friction loop data show that there was less tip-to-surface friction in the irradiated regions.

Figure 18. AFM analysis of the irradiated and unirradiated PtBuMA (top and photosensitive polyimides (bottom).

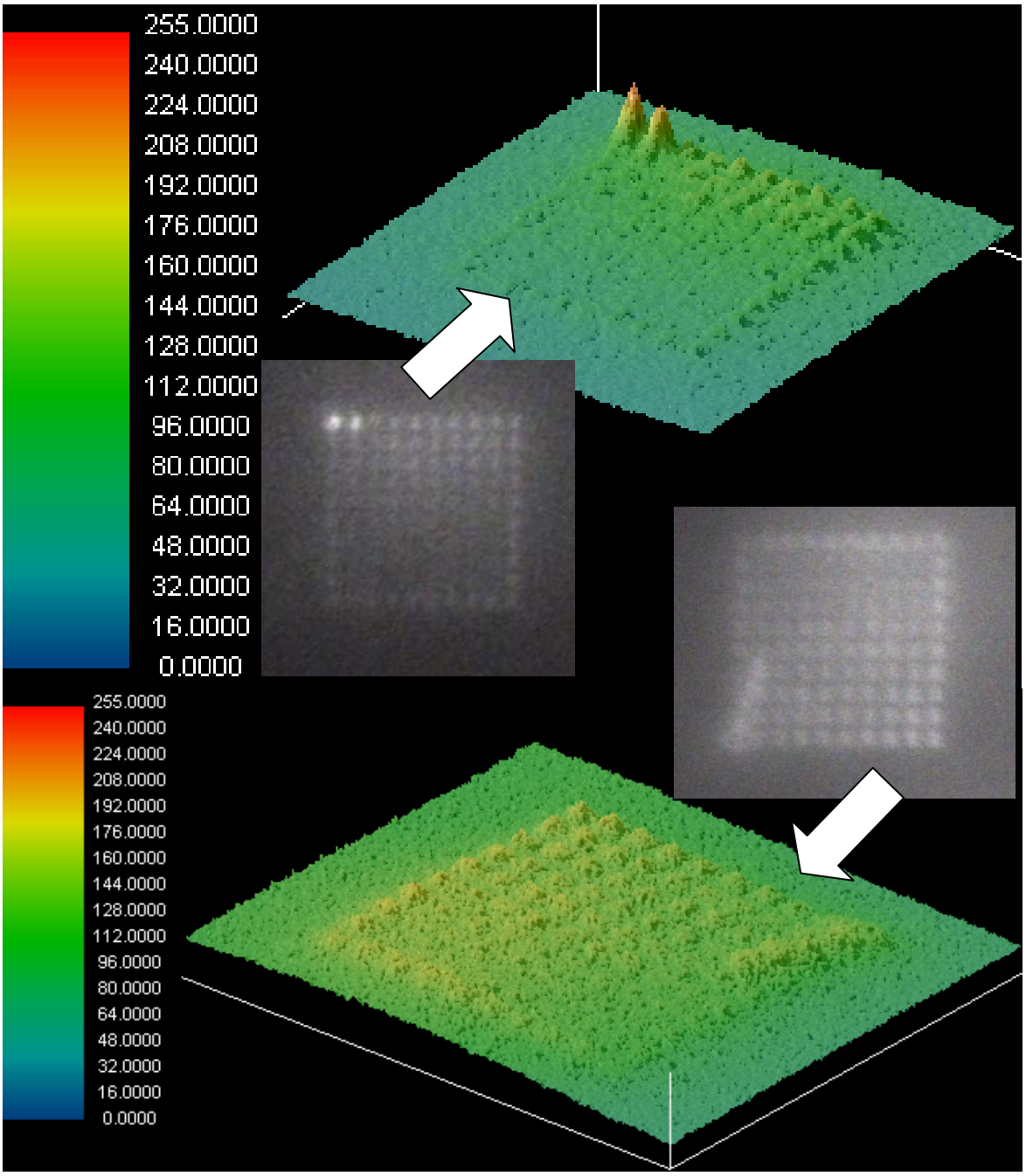

Figure 19. Relative mass of adsorbed hydrophobicity-sensitive protein (lysozyme, top); and hydrophobicity-'insensitive' protein (BSA, bottom) to variations in hydrophobicity in a microarray format. The polymer is AAPO exposed with different UV energies.

The difficulty of studies of protein adsorption on photopolymers arises from the difficult quantification. Usually fluorescence would be the most convenient method, but also usually, photopolymers have a fluorescent background. The photopolymers that photo-

react in the e-beam, or deep-UV region(s) would not have large fluorescence background, but would not have a 'rich' surface chemistry. The best experimental alternative is to use for the quantification of fluorescence (and hence the adsorbed protein) a confocal microscope (which will minimize the overall background from the polymer) with spectral imaging capability (which will allow the search) of "fluorescence windows" that have the minimum overlap between the fluorescence of the polymer and of the tagged protein. However, these instruments where not available at the time of application and presently there are only two vendors offering such systems (Leica and Zeiss). The PI's University will acquire one of these systems and use it to complete this part of research.

An alternative to this problem has been found through the use of photo/thermal ablation of very thin metallic films on thermo-labile polymers, as described in Section 3.3. Figure 20 presents the possible chemical pathways for obtaining the combinatorial surfaces in micro/nanostructures.

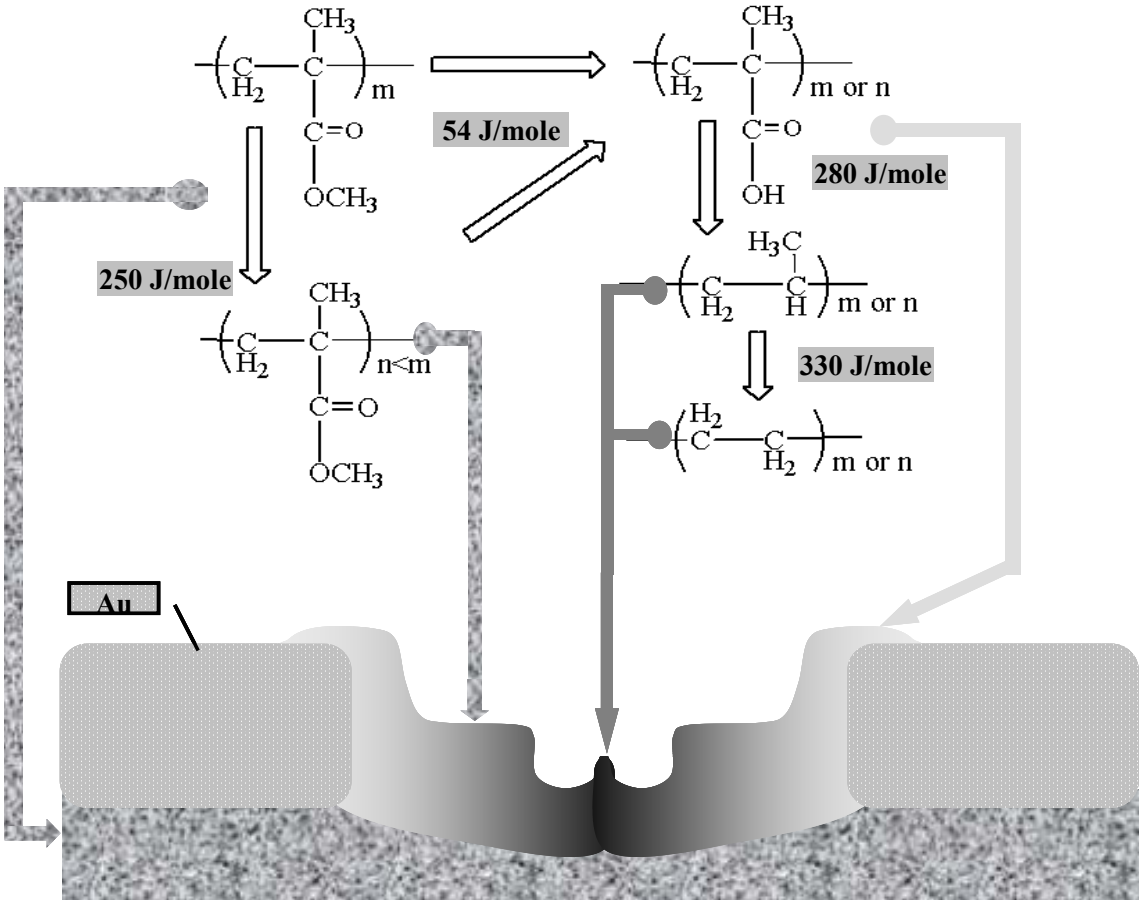

Figure 20. Photo-ablation induced thermal processes in confined spaces on top of polymeric (PMMA) layer. While the center of the microstructure is hydrophobic, the outer regions are hydrophilic. Different polymers, metals, thickness of the metallic layer and ablation energies/fluences will produce different combinatorial surfaces.

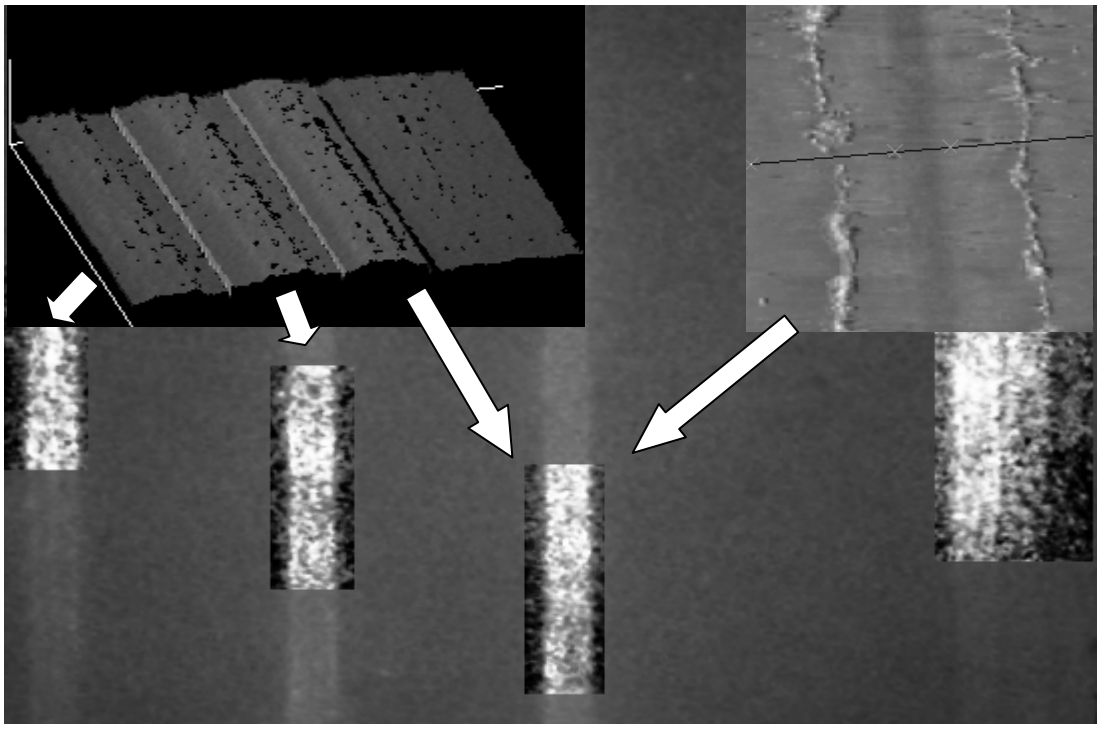

Figure 21. Spatially selective adsorption of proteins on micro/nanostructures. Image analysis of fluorescent images, versus corresponding topography/hydrophobicity measured with the AFM.

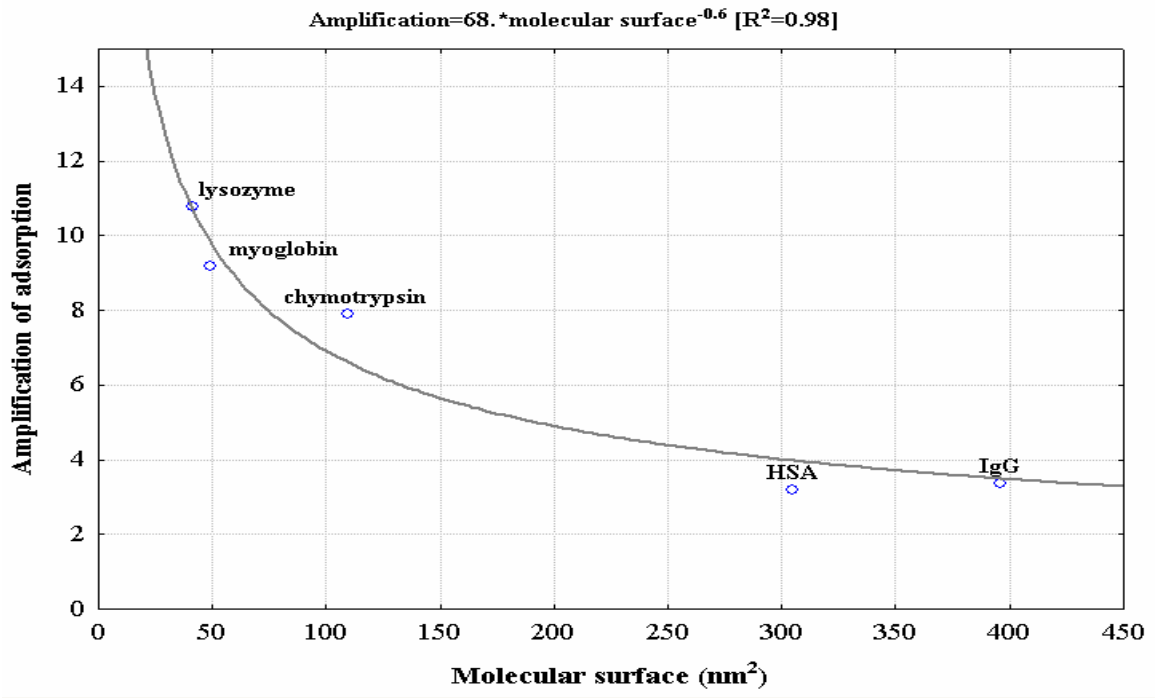

Figure 22. Amplification of protein adsorption on combinatorial micro/nano-structures.

The minimum amplification (~3x) is equivalent with the increase in specific surface. The process described above generates micro/nano-topographies with high reproducibility, comprising large variations of hydrophobicity, from highly hydrophobic (concentrated in the middle of the ablated area) to hydrophilic (at the edges) micro/nano-surfaces. The spatially selective (Figure 21) adsorption of protein is amplified from approximately 3-times for large proteins (presenting 'combinatorial' molecular surfaces themselves) to 12-times for small, simpler proteins (Figure 22).

The study proves the differential adsorption of e.g. proteins across a 'simulated' microfluidics channel, with the likelihood of clotting of the microstructures that present large variations of hydrophobicity confined in micrometer spaces, e.g. microfluidics corners.

4.4 Scaling relationships regarding biomolecule adsorption on polymeric surfaces

The fourth research module delivered scaling relationships that can be used for the design of microfluidics devices, in particular plastic-based devices.

4.4.1 Scaling relationships for polymer ablation

The first -minor- line of research focused on deriving scaling relationships for the ablation of polymers, a process that is increasingly used in the fabrication of microfluidics devices. The study aimed to seek a correlation between ablation rates and various polymer thermal properties, based on experimental ablation data generated for 14 polymers commonly used in microfluidics. A statistical analysis was carried out for laser fluence against various polymer descriptors and/or their combinations. The results of the analysis show a relatively high correlation coefficient of 0.82 for polymer ablation data when we compare fluence against the product of ablation rate and the difference between the glass transition temperature and room temperature. If the ablation rate is known for a 'base' polymer, then the following scaling relationship will give the ablation rate for the tested polymer:

$$AF \approx r\,[Cp\,(Tm - Tr) + \Delta H + \cdots] \qquad (4)$$

where A is the absorption coefficient of the laser energy by the polymer; F is the laser fluence (J cm−2); r is the ablation rate (μm/shot); Cp is the heat capacity (J mol^{-1} $°C^{-1}$); Tm is the melting temperature (°C); Tr is the room temperature (°C); and ΔH is the melting enthalpy (J mol^{-1}).

4.4.2 Testing the design limits of micro/nano-channels in microfluidics

'Lab-on-a-chip' microfluidics devices manipulate biological fluids, which contain significant quantities of biomolecules, in particular proteins and DNA, and even living cells. As the dimensions of these devices continue to decrease and approach the sub-micron range, and as the trend towards 'disposable' devices continues, the impact of the

inevitable adsorption of biomolecules becomes more important. Here, we estimated the protein-adsorption-related sensitivity of the geometry of a rectangular micron-sized channel. The estimation of the thickness of the adsorbed protein layer versus processing parameters, i.e. protein concentration in the fluid; ionic strength of fluid; and surface tension of the walls, is based on a proposed semi-empirical model for protein adsorption. The model, derived from the data contained in the biomolecule adsorption database, uses the concept of a 'generic protein', i.e. a protein with molecular properties averaged over the range of data present in the database.

The scaling relationships using a 'generic' protein use a multivariable linear relationship to mimic a Langmuir-Freundlich isotherm, as follows:

$$\Gamma = f_1(\gamma, ion\_str, abs(pH-pI), C)\cdot(1-g(\Gamma)) + f_2(\gamma, ion\_str, abs(pH-pI), C)\cdot g(\Gamma) \quad (5)$$

$$f_1 = a_{11}\gamma + a_{12}\cdot ion\_str + a_{13}\cdot abs(pH-pI) + a_{14}\cdot C + b_1 \quad (6)$$

$$f_2 = a_{21}\gamma + a_{22}\cdot ion\_str + a_{23}\cdot abs(pH-pI) + a_{24}\cdot C + b_2 \quad (7)$$

$$\Gamma < \Gamma_{breakpoint} \Rightarrow g(\Gamma) = 0 \quad (8)$$

$$\Gamma \geq \Gamma_{breakpoint} \Rightarrow g(\Gamma) = 1 \quad (9)$$

where Γ is the protein surface concentration (mg/m^2); C is the protein concentration in solution (mg/ml); γ is the surface tension of the polymer (dyne/cm); ion_str is the ionic strength (M); pI is the protein isoelectric point; $\Gamma_{breakpoint}$ is the protein concentration at which the slope of the linear function Γ = f(C) changes; and the rest of the parameters are constants, as shown in Table 2.

Table 2. Coefficients for the protein adsorption (Equation above).

	Surface tension (dyne/cm)	Ionic strength (M)	Abs(pH-pI)	Protein concentration in solution (mg/ml)	Free term
Coef. in f_1	a_{11}=0.076	a_{12}=-3.297	a_{13}=0.085	1.052	b_1=4.44
Coef. in f_2	a_{21}=-0.014	a_{22}=3.701	a_{23}=-0.395	0.438	b_2=4.84
Mean	44.82892	0.07505	1.39033	0.49182	
Standard deviation	6.942584	0.071997	0.914402	0.760767	
Break point for the protein surface concentration (mg/m^2)					3

Figure 23 presents the predicted evolution of the thickness of an adsorbed protein layer; and subsequent variation in the pressure drop; versus operational parameters. The operational parameters have been tested in pairs, i.e. protein concentration in solution (a key parameter in protein adsorption); and surface tension of the polymer (material descriptor); and ionic strength of the solution (medium descriptor); respectively.

From this analysis, i.e. the estimation of protein-adsorption-related impact on the geometry of a rectangular micron-sized channel, i.e. narrowing of the micro-channel, it appears that the values (i.e. protein thickness and variation of the pressure drop – Newtonian fluid) vary dramatically below a threshold value of approximately 1.5-2 μm. Several key parameters can vary dramatically from case to case, i.e. protein nature; and several assumptions could be easily challenged, e.g. the Newtonian character of the fluid, especially at high protein concentrations. The study gives however the 'bottom line' of the design security zone where simple design principles can be used. Further more in depth analysis, including molecular descriptors of the protein, follows in the next subsection.

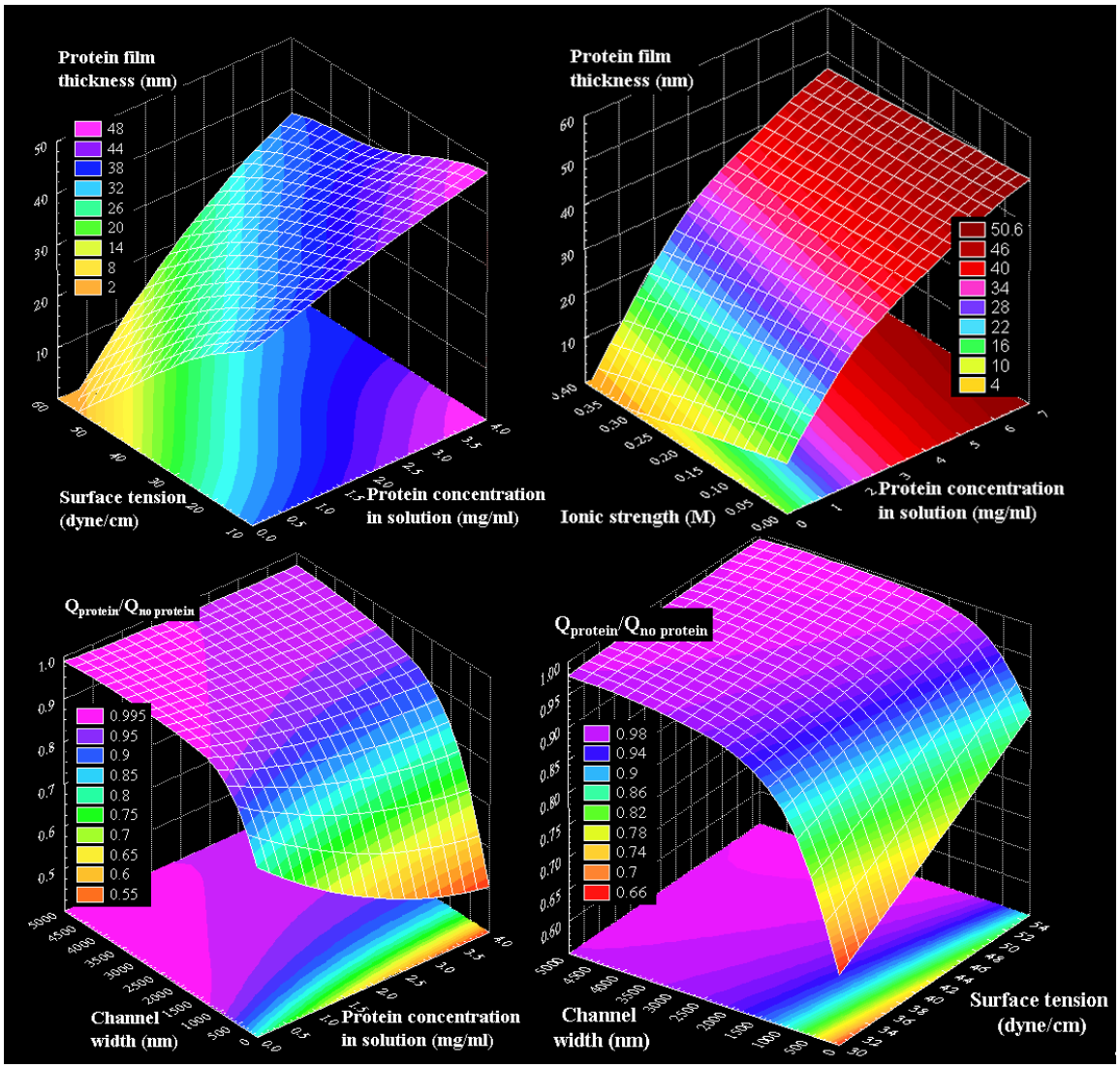

Figure 23. Variation of the thickness of an adsorbed protein layer; and pressure drop in microchannels, function of protein concentration in solution; surface tension of the polymer; and ionic strength of the solution, respectively.

4.4.3 Calculation of protein surface descriptors

These algorithms are based on an extension of the well-known Connolly algorithm. The rationale behind this method of computation of the solvent-accessible surface of a molecule is that the only parts of the surface that are smaller than or around the same size as the solvent molecules actually interact with the latter: smaller "clefts" are not geometrically accessible. Based on this idea, Connolly's algorithm rolls an imaginary sphere of a radius close to the effective radius of a solvent molecule (in the case of water, 1.4 Å) over the 3-dimensional structure of the molecule under analysis, recording the contact points of this ball with the van der Waals spheres representing the constituent atoms of the latter. Together, these "pivot" points represent a good approximation to the solvent-accessible surface. We extended this algorithm by assigning either to each atom or to each amino acid of a protein a real number representing some property of that atom or residue, for example charge or hydrophobicity. Then, while rolling the solvent sphere over the structure of the protein, we sum the values of the parameter of interest encountered at each pivot point on the surface. The result of this summation is an approximation to the integral of the parameter over the solvent-accessible surface. We implemented these algorithms in a freely available Windows™ program which we call the Protein Surface Properties Calculator (freely available at www.bionanoeng.com). Figure 24 presents a map of the charges on the surface of a protein, probed with two radii.

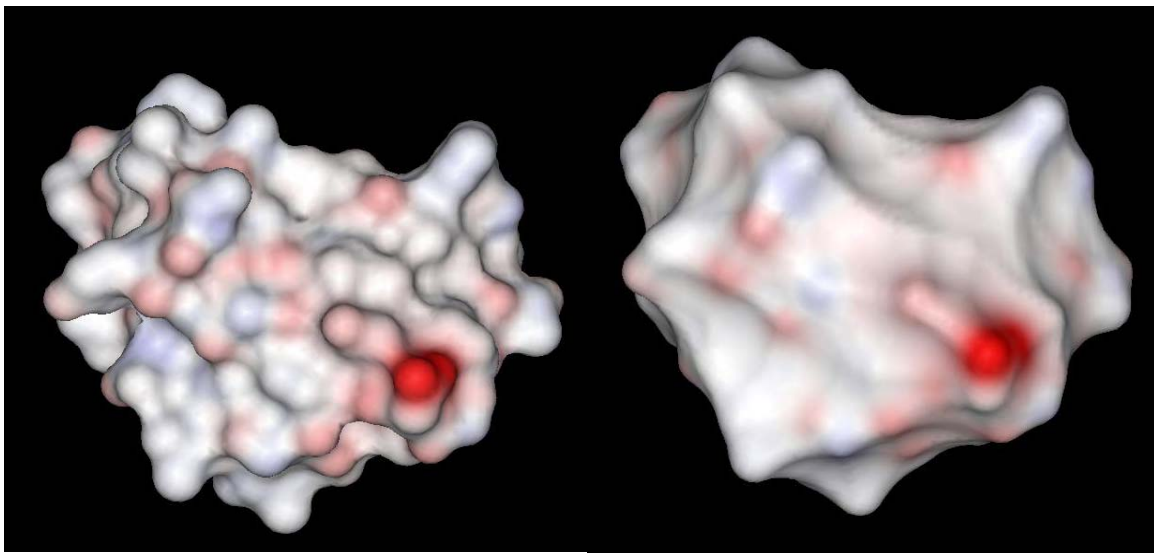

Figure 24. Water-accessible, i.e. probe radius=1.4Å (left) and plane-accessible, i.e. probe radius=∞ (right) charge surfaces of the same protein (crambin).

As opposed to charges, the hydrophobicity cannot be easily assigned to individual atoms. For example, all hydrophobicity scales use an amino-acid scheme while charge is a fundamental property of an atom rather than a set of atoms. However, the assignment of properties to entire residues, while meaningful, presents some problems, especially in the context of protein adsorption on surfaces. Among these is the resulting assumption that

the value of the parameter of interest is distributed homogenously across the residue's solvent accessible surface, which is not at all reasonable. Another drawback is that the best spatial resolution one can obtain is limited by the dimensions of a residue. These and other motivations led us recently to propose a scheme for converting residue-based properties to atomic properties via a linearity approximation (i.e. the value of a parameter over a residue is equal to the sum of the unknown properties of the constituent atoms, possibly scaled by the exposed areas of these).

Although the assignment of physico-chemical parameters to individual atoms is not always physically meaningful (as is the case with hydrophobicity), it is more robust and can give numerically superior results. We showed that mapping residue-based hydrophobicity scales to atomic ones leads to a more meaningful clustering of proteins and reveals atomic-resolution surface features that could not be determined by the amino-acid assignment alone. Consequently, we used this method to map the Kyte-Doolittle hydrophobicity scale to individual atoms based on a scheme involving 12 different atomic types (atoms were grouped by chemical similarity). It was this measure that was used to compute the surface of hydrophobicity and hydrophilicity.

The superiority of our atom-based hydrophobicity method, as opposed to the amino-acid based hydrophobicity, especially in the context of protein adsorption, appears when we classify several proteins according to their overall characteristics of the molecular surface. Figure 25 presents the clustering of 42 very different proteins using different classification methods.

The classification using atomic properties (e.g. charges, Figure 25 top left) can distinguish between different protein types with blue (approximate) rectangles representing similar PDB structures for classes of proteins, i.e. amine oxidase; α-lactoglobulin; lysozyme; ribonuclease-A; haemoglobin; α-chymotrypsin; actin-gelsolin and actin-profilin; myosin; serum albumin; and immunoglobulin. The best resolved cluster (in the middle) represents 8 very similar structures of haemoglobin. In contrast with this validated clustering, the classification based on amino-acid based hydrophobicity cannot resolve the well defined haemoglobin in cluster, but rather lumps all proteins in two very general clusters. However, both atomic-based hydrophobicities (Figure 25 bottom row) when used to cluster proteins according to their overall molecular surface properties are capable to classify the 42 proteins with similar accuracy as charge-based classification. As hydrophobicity, much more than charges, has an important impact on protein adsorption, it was expected that this method of quantification of molecular surface properties will lead to greater accuracy in predicting protein adsorption. Moreover, this method can be used to better classify the similarity of protein pairs, and infer adsorption data for an untested protein from the existent data in the adsorption database.

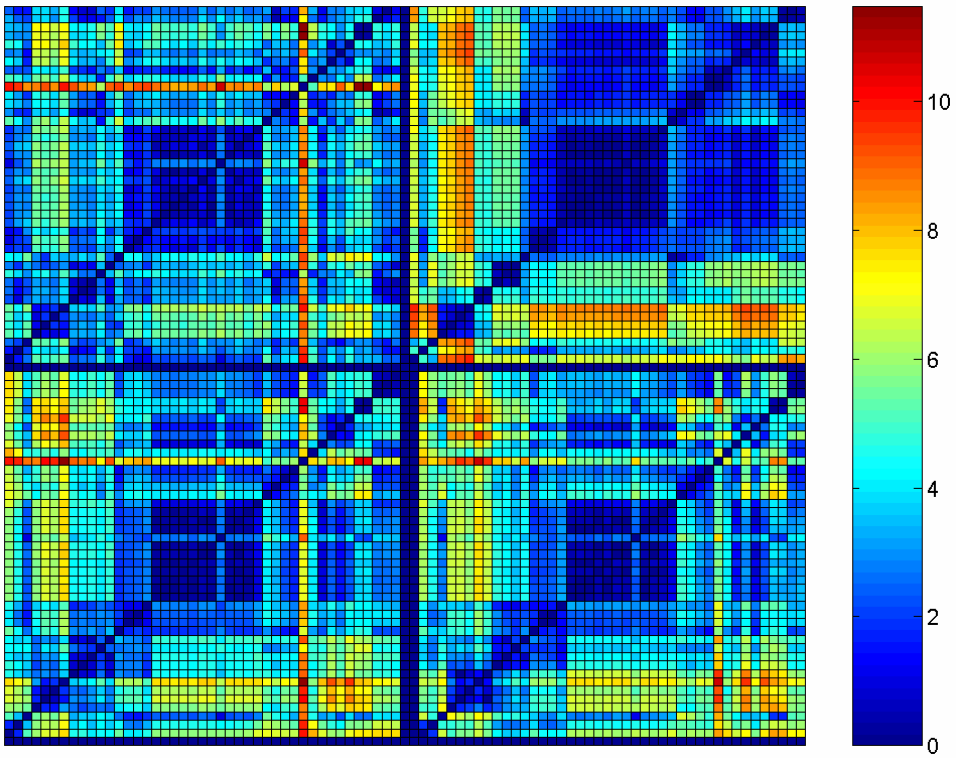

Figure 25. Clustering of 42 proteins according to molecular surface descriptors, calculated using charges (top left); amino-acid based hydrophobicities (top right); atomic-based hydrophobicity based ignoring the atomic solvent accessible area (ASA) (bottom left); and taking ASA into consideration (bottom right). The colored scale of dis/similarity is presented on the right, with dark blue meaning identical cases.

We also worked on the charges-based descriptors. When representing the electrostatic potential, quite often the charges are fixed and independent of pH. To determine the charges on the atoms in each protein, we used semi-empirical methods (we used PM3 method which is quite robust and verified) on each amino acid terminated by two different identical residues at each end to determine the charges on the constituent atoms of the central amino acid. We make the assumption that the effect of more distant residue bonds and that due purely to different locations in a folded protein to be negligible. The resultant charges were used to compute surface charge properties for each protein in the data set.

4.4.4 Prediction of protein adsorption - a QSAR approach

The parameters calculated with the method described above for each of the tested proteins are listed in Table 3. Clearly, these are not all mathematically independent of each other, and some are even directly related or linear combinations of one another (e.g. the total area equals the sum of the positively and negatively charged areas). Thus, we attempted to select an appropriate subset of parameters from this table to use for the final model fitting. In addition to these, we also used the principal descriptors of the

environment and adsorbing surface, available from the BAD: protein bulk concentration in mg/ml, pH of the solution, ionic strength of the solution in mM and the surface tension of the adsorbing surface in dynes/cm. The isoelectric point of each protein was calculated using HyperChem. As the temperature used for the measurements in the final data set was almost always very close to room temperature, this variable was not included.

Table 3. Surface descriptors (areas are in Å^2 and "specific" means scaled by total or respective surface area).

Symbol	Meaning
Area	Surface Area
PosArea	Positive Surface Area
PosCh	Total Positive Charge
NegArea	Negative Surface Area
NegCh	Total Negative Charge
TotCha	Total Charge at the Surface
HyPhiA	Hydrophilic Area
HyPhoA	Hydrophobic Area
TotHypho	Total Surface Hydrophobicity
TotHyPhi	Total Surface Hydrophilicity
SpPosA	Specific Positive Area
PosChDen	Surface Positive Charge Density
SpPosChD	Specific Positive Charge Density
SpNegA	Specific Negative Area
NegChDen	Surface Negative Charge Density
SpNegChD	Specific Negative Charge Density
SpHphiA	Specific Hydrophilic Area
HphiDen	Hydrophilicity Surface Density
SpHphiD	Specific Hydrophilic Surface Density
SpHphoA	Specific Hydrophobic Area
HphoDen	Hydrophobicity Surface Density
SpHphoD	Specific Hydrophobic Surface Density

We obtained structure files for the tested proteins from the PDB databank at www.pdb.org. We then used the Protein Surface Properties Calculator to compute the

surface parameters listed in Table 3. The probe radius used was 100 Å. The reason for using this very large value instead of the customary 1.4 Å is that in the interaction of a protein with a surface (which is what controls adsorption) it is not the surface accessible to a water molecule which matters, but the surface accessible to an infinite plane representing the adsorbing surface. In the limit as $r \to \infty$, probing a protein structure with a sphere of radius r would clearly give the "plane-accessible" surface area of a molecule. The solvent-accessible and plane-accessible surfaces of a molecule are actually very different, as previously illustrated in Figure 24. We have found that surface parameters computed using large probe radii are more strongly correlated with adsorbed amounts than are those computed using smaller probe radii, and this difference represents around 30% of the correlation coefficient for most of those parameters.

We attempted to fit the data to a piecewise linear model with a breakpoint. This is in a sense the simplest non-linear model. Let the dependent variable be v_0 and the independent variables used in the model be v_1, v_2, …, v_n. Then according to a piecewise linear model with a single breakpoint b

$$\begin{cases} v_0 = \sum_{i=1}^{n} b_{1i} v_i, v_0 \le b & (10) \\ v_0 = \sum_{i=0}^{n} b_{2i} v_i, v_0 \ge b & (11) \end{cases}$$

where the b_{1i} are the parameters of the model for the region before the breakpoint i.e. $v_0 \le b$ and the b_{2i} are the corresponding parameters for $v_0 \ge b$. Additionally, we have the condition that the model must be continuous, i.e. at $v_0 = b$, both expressions take the same value.

In essence, this model works with the assumption that there are two different "regimes" for the dependence of v_0 on the other variables. Protein adsorption is known to be non-linear in time, bulk concentration and other variables. At low concentrations of protein in solution or under unfavorable conditions, protein adsorption is generally diffusion-limited. At higher concentrations and favorable conditions (e.g. high affinity of the protein for the adsorbing surface) the process is limited by the surface's finite capacity for adsorption. Hence there are strong reasons to suspect that the assumption of more than one regime of adsorption is well-founded, and thus that this model will be a much more appropriate one than a simple multiple linear regression.

Table 4. Parameters in Equations 10 & 11.

Coefficient of Parameter	Value before breakpoint	Value after breakpoint
Free term	9.020827	-0.79537
Bulk Concentration	0.169786	0.390651
Surface Tension	-0.04516	-0.01666
pH	-1.13612	-0.03771
Ionic Strength	-0.88226	-2.00472
Isoelectric Point	0.345245	0.376041
Surface Area	-3.5E-05	-2.5E-05
SpPosChD	125.4071	356.3409
SpNegChD	-312.176	-152.826
SpHphiD	-220.843	-142.063
SpHphoD	-707.82	-464.124

We used the package Statistica™ with the data set defined in Table 4 including the surface and environment parameters. This model was evaluated using a least-squares penalty function. The breakpoint is estimated manually, since we found that this gives better fits than allowing the algorithm to estimate it. The optimization used several different estimation algorithms, with convergence criterion set to 10^{-5}. The plot of observed against predicted values is shown in Figure 26. Note the apparent "gap" near the area where the breakpoint was applied.

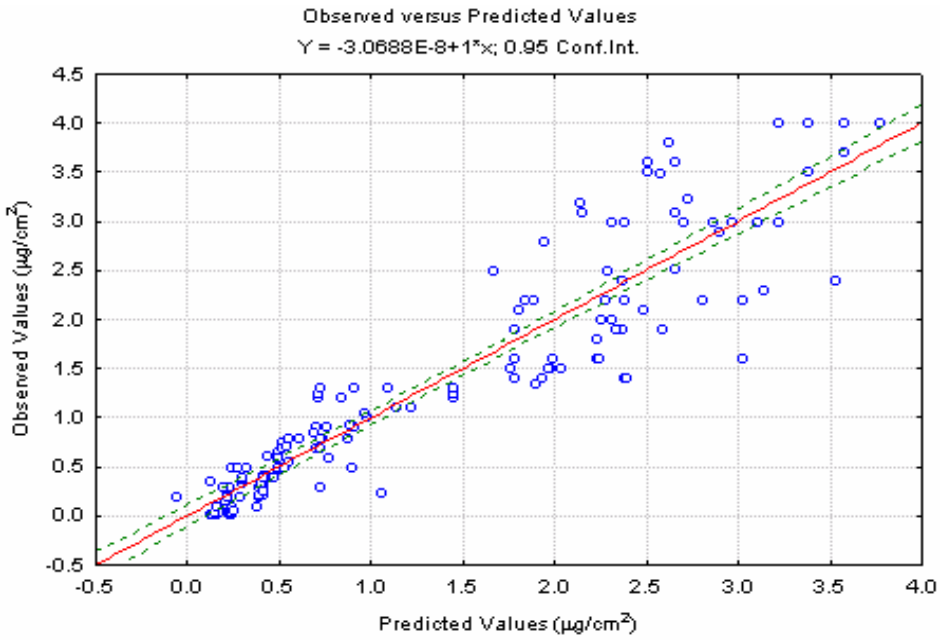

Figure 26. Comparison of the predicted (piece linear regression with breakpoint) and observed data (from BAD) for protein adsorption.

Figure 27 shows the normal plot of the residuals. Note that these are close to normal (i.e. the plot is approximately linear). The absence of any significant pattern about the "normal line" is an indication that the model is appropriate in the sense that no significant parameters have been omitted (as this would have caused the residuals to be non-normally distributed).

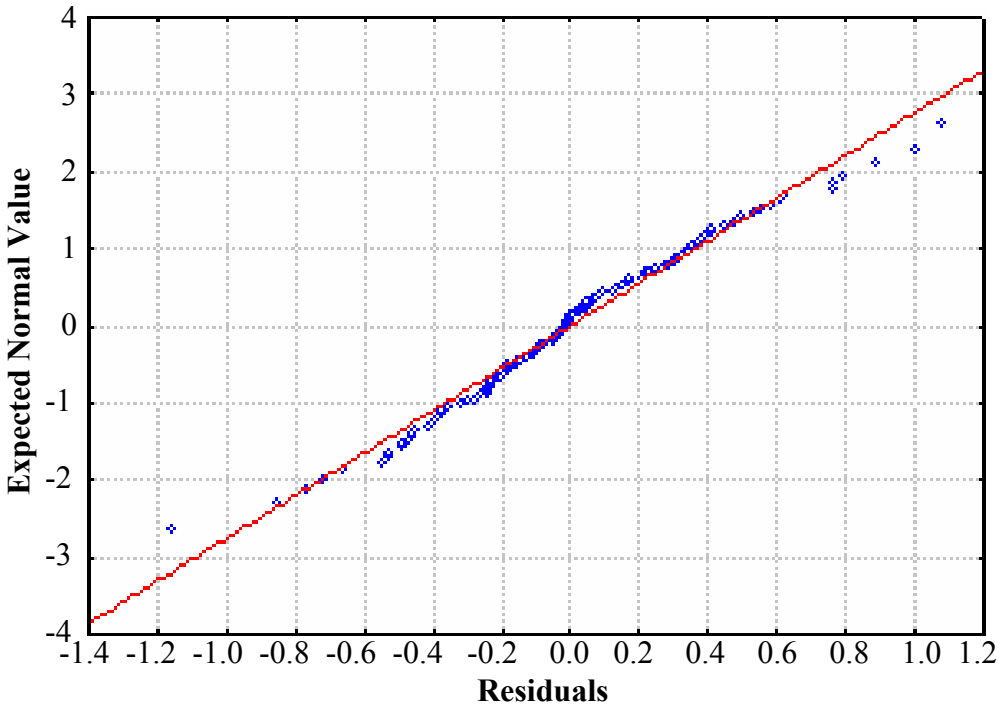

Figure 27. Normal probability plot of residuals. Note that the plot is almost linear.

Quite aside from the inherent physical complexity of the protein adsorption process itself, some of the parameters in the data set vary over several orders of magnitude. For example, the bulk concentration of protein in even the reduced data set used for fitting is as low as 0.001 mg/ml and as high as 10 mg/ml (4 orders of magnitude). The adsorbed amount and the ionic strength of the solution also show a similar degree of variability. Thus, it is not surprising that one linear regime is not enough to describe continuously the data in question. What is surprising is that only two linear regimes suffice to produce a good fit. Given that the literature data is not always consistent and that realistically, the uncertainty in determining the concentration of protein at the surface is in most cases at least 10% if not more, it is quite surprising that any model can meet with such success, even a purely empirical one. Even if we relax the condition that the adsorbed amount be below 4 $\mu g/cm^2$, the piecewise linear model still explains no less than around 76% of the variation in the data while the optimal breakpoint is found in this case to be no higher than around 2.5 $\mu g/cm^2$.

We investigated whether varying the breakpoint would have a significant impact on the quality of the fit. The results are shown in Figure 28. Note that the difference between using breakpoints as low as 1.2 μg/cm^2 and as high as 2.4 μg/cm^2 compared to the optimal 1.7 μg/cm^2 is not great. This could be taken as an indication of the degree of "health" in the model, since it is clear that the breakpoint value is not due primarily to artifacts in the data.

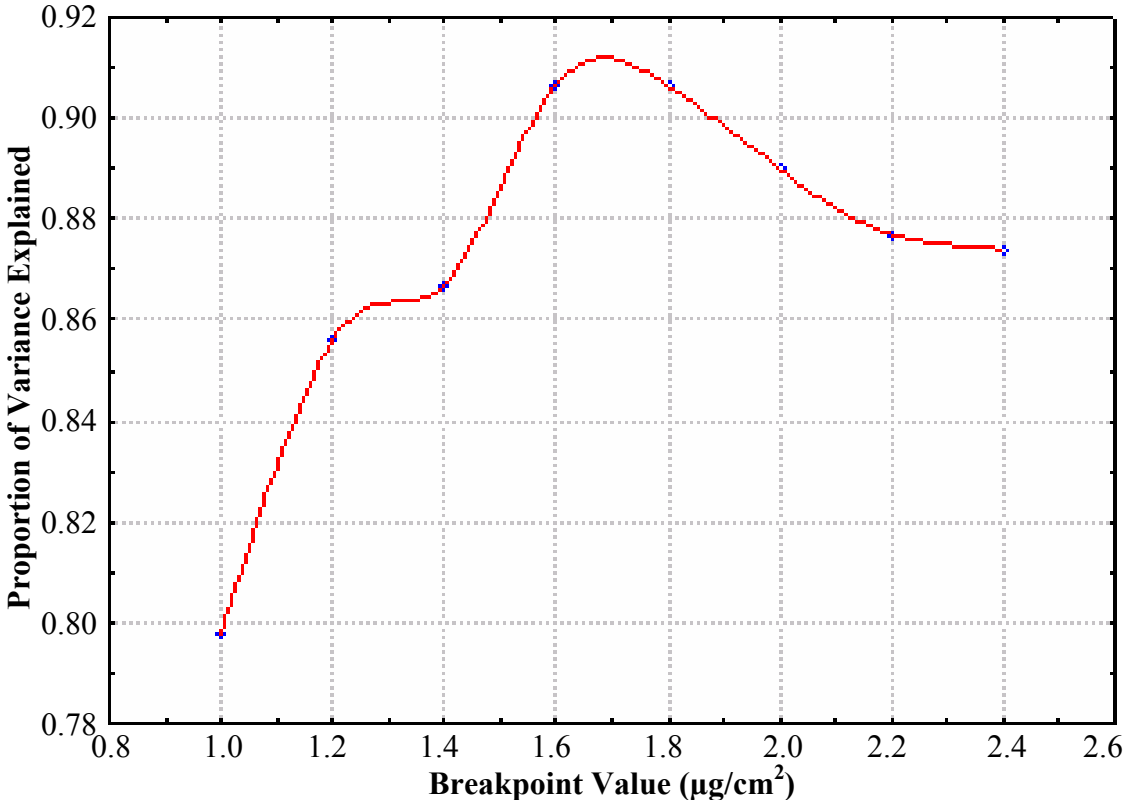

Figure 28. Proportion of variance explained vs. breakpoint value. The variation of the fit of the model with a manually set breakpoint value (note the maximum around 1.7μg/cm^2).

The use of an empirical model such as this does not -in general- have any theoretical implications for a phenomenon. However, all parameters in Table 4 are physically meaningful. For instance, the increase in ionic strength decreases the adsorbed amount of protein, especially after few monolayers have been deposited on the surface. On the other hand, the ability to predict protein adsorption to surfaces from solution over such a wide range of conditions, proteins and surfaces is very useful for pragmatic reasons and finds applications in biomedicine and other areas, let alone as design tools for microfluidics devices.

5.0 Conclusions

The project "SCALING RELATIONSHIPS FOR BIOMOLECULES ADHESION AND ACTIVITY ON POLYMERIC SURFACES" has focused on the understanding, quantification and derivation of scaling relationships regarding the attachment of biomolecules and cells on polymeric surfaces. The initial scope of the project, which included the attachment of biomolecules (with emphasis on proteins) was augmented in the later stages of the project with the inclusion of attachment of cells, in particular bacterial cells. The project aimed to deliver design tools that can be used in the process of design, fabrication and operation of microfluidics devices, in particular plastic-based devices.

The main deliverables and findings of the project can be articulated as follows:

Database for biomolecular adsorption. The database, which is freely accessible at www.bionanoeng.com/bad/, comprises a few hundred cases of protein adsorption on different materials. The database is organized along surface descriptors (surface tension and contact angle); environment descriptors (pH; ionic strength; and temperature); and protein descriptors. The molecular descriptors regarding the protein (or any other biomolecule) are calculated with an in-house developed software package (freely available at the same site). The site, comprising the database and a downloadable version of the software, has been used by many thousands of researchers and is visited few hundred times per week over the period of the last 2 years. The database will be maintained in the future with funds from the proposing University.

Atomic Force Microscopy studies of biomolecular and cell attachment on polymers. Atomic Force Microscopy (AFM) was used to measure the attraction/repulsion forces between 'model' amino acids mounted on an AFM tip and 'model' surfaces. These fundamental parameters are in the process of being implemented in a model of protein adsorption, which will also use the database for biomolecular adsorption as a base for parameterization and validation. Also, AFM experiments focused on the structure of the proteins and DNA; and bacterial cells on several polymeric surfaces. It has been found that the polymer surface modulates the molecular structure of the DNA molecules and hence the hybridization process. It has also been found that philogenetically close-related bacterial species have quasi-identical response towards polymeric hydrophilic surfaces (repelled); but exhibit enormously different metabolic response towards hydrophobic surfaces. These results are useful to a better selection of polymers for microfluidics applications.

Adsorption of biomolecules on combinatorial surfaces. Several photosensitive polymers demonstrated the selective attachment of proteins, but the best option was to fabricate the combinatorial surfaces using a process (now patented) that uses the ablation of a very thin layer of metal to process thermally and in-situ the top surface of an underlying thermo-labile polymer substrate. This process generates micro/nano-topographies with high

reproducibility, comprising large variations of hydrophobicity, from highly hydrophobic (concentrated in the middle of the ablated area) to hydrophilic (at the edges) micro/nano-surfaces. The adsorption of protein is amplified from approximately 3-times for large proteins (presenting 'combinatorial' molecular surfaces themselves) to 12-times for small, simpler proteins. The study proves that the differential adsorption, of e.g. proteins, across a 'simulated' microfluidics channel, with the likelihood of clotting of the microstructures, presents large variations of hydrophobicity confined in micrometer spaces, e.g. microfluidics corners.

Scaling relationships regarding biomolecule adsorption on polymeric surfaces. The fourth research module delivered scaling relationships that can be used for the design of microfluidics devices, in particular plastic-based devices. The first -minor- line of research focused on deriving scaling relationships for the ablation of polymers, a process that is increasingly used in the fabrication of microfluidics devices. The second -major- line of research used the Biomolecular Adsorption Database and protein molecular descriptor software (developed under research module 1) to derive relationships that link directly a parameter related to biomolecular adsorption (e.g. height of the adsorbed layer in nm) to (i) molecular descriptors of the adsorbed biomolecule (e.g. % hydrophobic surface; specific hydrophobicity; etc. – up to 18 relevant descriptors); (ii) environment conditions (e.g. pH and ionic strength; coupled with biomolecular 'global' properties, e.g. isoelectric point); and (iii) surface descriptors (i.e. surface tension/contact angle). For the data available, the correlation fit reached 80-90%, depending on the range of variables. These scaling relationships have been used, for instance, to prove that protein adsorption on the walls of micro-channels cannot be ignored when designing microfluidics devices for widths of the channels smaller than 1.5-2 microns.

Several *key performance indicators* of the project are as follows:

- 13 journal papers published or in print; and 2 other submitted or in the process of submission;
- 19 conference full papers
- 1 database and 1 software package;
- 1 patent and associated commercialization effort;
- 2 explicit collaborative efforts, one within Bioflips program; one within Simbiosys program.

6.0 Recommendations

The research findings point to several future avenues of research, organized along the four research modules, as follows:

Database for biomolecular adsorption. Further work is recommended regarding the expansion of the database; and the upgrade of the computer software that calculates the molecular descriptors of the biomolecules with a visualization capability. Both products are close to being translated into commercial products, preferably to a specialized company (e.g. CFDRC); but alternatively through a spin-off software company.

Atomic Force Microscopy studies of biomolecular and cell attachment on polymers. Further work is necessary regarding the measurement of the attraction/repellent forces between all amino-acids (presently only four have been quantified); and four DNA bases as well as other small biomolecules; and combinatorial surfaces. Alternatively, quantum mechanics calculations can be performed in association with a shorter list of AFM measurements, with which the simulations will be calibrated against. The simulations will constitute a direct input into the molecular descriptors software (described above). A different line of research regarding the surface-modulated metabolic response of the bacteria, and its possible relationship with pathogenesis, would also be desirable.

Adsorption of biomolecules on combinatorial surfaces. Additional work is needed to translate the concept of combinatorial surfaces for the probing of bioactivity of surface-immobilized biomolecules into practical devices – an objective that was outside the scope of the initial proposal. The projected benefits of a microarray device based on combinatorial surfaces are better (around 3-10 times higher) detection sensitivity; less variability of the detection levels; and easy and intuitive information 'bar-code'-wise encoding in microstructures.

Scaling relationships regarding biomolecule adsorption on polymeric surfaces. Further work is needed to bring the concept of scaling relationships in 'turn-key' software, possibly packed with the database and the software for the calculation of molecule descriptors. More work would be needed to transform the parameters of the empirically fitted scaling relationships in parameters with clear physical meaning.

7.0 References

7.1 Journal papers

1. G. S. Watson, J. A. Blach, C. Cahill, D.V. Nicolau, D. K. Pham, J.P. Wright, S. Myhra. Interactions of poly(amino acids) in aqueous solution with charged model surfaces - analysis by colloidal probe. *Biosensors & Bioelectronics* (accepted).
2. E.P. Ivanova, D.K. Pham, N. Brack, P. Pigram, D.V. Nicolau. Poly(L-lysine)-mediated immoblisation of oligonucleotides on carboxy-rich polymer surfaces. *Biosensors & Bioelectronics* (accepted).
3. Nicolau, D. V. Jr., Fulga, F., Nicolau, D. V. Impact of protein adsorption on the geometry design of microfluidics devices. *Biomedical Microdevices* 5 (3), 227-233, 2003.
4. Nicolau, D.V. Jr., Fulga, F., Nicolau, D.V. A new program to compute the surface properties of biomolecules. *Asia-Pacific Biotech*, 7(3) (Special Issue: "Bioinformatics in Asia Pacific") 29–34, 2003 (also Proceedings of the 1st Asia-Pacific bioinformatics conference on Bioinformatics, 19, 2003.
5. Watson, G.S., Blach, J.A., Cahill, C, Nicolau, D.V., Pham, D.K., Wright, J., Myhra, S. Poly(amino acids) at Si-oxide interfaces—bio-colloidal interactions, adhesion and 'conformation'. *Colloid and Polymer Science* (published on line: http://www.springerlink.com/)
6. Watson, G.S., Blach, J.A., Nicolau, D.V., Pham, D.K., Wright, J.P., Myhra, S. Surface topography and surface chemistry of radiation-patterned P(tBuMA) - analysis by atomic force microscopy. *Polymer International,* 52, 1408, 2003.
7. Wright, J.P., Ivanova, E., Pham, D.K., Filipponi, L., Viezolli, A., Suyama, K., Shirai, M., Tsunooka, M., Nicolau, D.V. Positive and Negative Tone Protein Patterning on a Photo-base Generating Polymer. *Langmuir*, 19(2); 446-452, 2003.
8. Cao, J., Pham, D.K., Tonge, L., Nicolau, D.V. Predicting surface properties of proteins on the Connolly molecular surface. *Smart Materials & Structures,* 11 (5) 772-777, 2002.
9. Ivanova, E. P., Papiernik, M., Oliveira, A. M., Grodzinski, P., Nicolau D. V. Feasibility of polystyrene-derived polymeric surfaces for covalent attachment of the oligonucleotides. *Smart Materials and Structures* 11 (5) 783-791, 2002.
10. Ivanova, E., Wright, J.P., Pham, D.K., Filipponi, L., Viezolli, A., Nicolau, D.V. Polymer Micro-structures Fabricated via Laser Ablation for Multianalyte Microassays. *Langmuir*, 18, 9539-9546, 2002.
11. Cao, J., Pham, D. K., Tonge, L., Nicolau, D. V. Study of atomic force microscopy force-distance curves by simulation using the Connolly surface for proteins. *Smart Materials & Structures,* 11 (5) 767-771, 2002.

12. Ivanova, E. P., Pham, K.D., Wright, J., Nicolau, D.V. Detection of coccoid forms of *Sulfitobacter mediterraneus* using atomic force microscopy. *FEMS Microbiology Letters* 214 (2), 177-181, 2002.
13. Tonge, L., Cao, J., Pham, D. K., Wright, J. P., Harvey, E. C., Nicolau, D. V. Effects of polymer properties on laser ablation behaviour. *Smart Materials & Structures,* 11 (5) 668-674, 2002.

7.2 Chapters in books

Nicolau D. V. Substrates and surfaces for microarrays. In Muller, U., Nicolau, D. V. (Eds.) Microarray Technology: Fundamentals, Fabrication and Applications. Springer Verlag 2003 (accepted for publication – January 2003).

7.3 Patents

Dan V. Nicolau, Elena Ivanova, Duy Pham and Jonathan Wright. Combinatorial micro/nano-surfaces for informationally-addressable microarray. Australian Provisional Patent 2002952384; International Patent Pending.

7.4 Databases

Dan V. Nicolau, Jr., Dan V. Nicolau. Biomolecule Adsorption Database. URL: http://www.bionanoeng.com/BAD

7.5 Programs

Protein Surface Properties Calculator (PSPC). URL: http://www.bionanoeng.com/BAD

7.6 Conference papers

1. Duy K Pham, Jonathan P Wright, Elena P Ivanova, Dan V Nicolau. AFM analysis of the polymer microstructures used for novel multianalyte protein microassay. Proc. SPIE Vol. 4966, 83-91, Microarrays and Combinatorial Technologies for Biomedical Applications: Design, Fabrication, and Analysis; Dan V. Nicolau, Ramesh Raghavachari; Eds., 2003.

2. Elena P Ivanova, Andrea Viezzoli, Yulia V Alekseeva, Gregory M Demyashev, Dan V Nicolau, Luisa Filipponi, Duy K Pham, Dan V Nicolau. Immobilization of multiple proteins in polymer microstructures fabricated via laser ablation. Proc. SPIE Vol. 4966, 37-49, Microarrays and Combinatorial Technologies for Biomedical Applications: Design, Fabrication, and Analysis; Dan V. Nicolau, Ramesh Raghavachari; Eds., 2003.

3. Duy K Pham, Elena P Ivanova, Jonathan P Wright, Dan V Nicolau. AFM analysis of the extracellular polymeric substances (EPS) released during bacterial attachment on polymeric surfaces. Proc. SPIE Vol. 4962, 151-159, Manipulation and Analysis of Biomolecules, Cells, and Tissues; Dan V. Nicolau, Joerg Enderlein, Robert C. Leif, Daniel L. Farkas; Eds., 2003

4. Luisa Filipponi, Elena P Ivanova, Andrea Viezzoli, Dan V Nicolau. Protein interaction with combinatorial structures. Proc. SPIE Vol. 4937, p. 84-89, Biomedical Applications of Micro- and Nanoengineering; Dan V. Nicolau; Ed., 2002

5. Jolanta A Blach, Gregory S Watson, Chris L Brown, Duy K Pham, Jonathan P Wright, Dan V Nicolau, Sverre Myhra. Nanolithography of polymer surfaces by Atomic Force Microscopy. Proc. SPIE Vol. 4937, 285-293, Biomedical Applications of Micro- and Nanoengineering; Dan V. Nicolau; Ed., 2002.

6. Gregory S Watson, Jolanta A Blach, Colm Cahill, Dan V Nicolau, Duy K Pham, Jonathan P Wright, Sverre Myhra. Interactions of poly(amino acids) in aqueous solution with charged model surfaces- analysis by colloidal probe Proc. SPIE Vol. 4937, 274-284, Biomedical Applications of Micro- and Nanoengineering; Dan V. Nicolau; Ed., 2002.

7. Elena P Ivanova, Duy K Pham, Gregory M Demyashev, Dan V Nicolau. Oligonucleotide/poly(l-lysine) complexes attachment on poly(styrene/maleic acid) and poly(styrene/maleic anhydride) polymeric surfaces Proc. SPIE Vol. 4937, 23-33, Biomedical Applications of Micro- and Nanoengineering; Dan V. Nicolau; Ed., 2002.

8. Dan V Nicolau, Jr., Dan V Nicolau Effect of Protein Adsorption on Fluid Flow in a Micro-channel Proc. SPIE Vol. 4937, 150-157, Biomedical Applications of Micro- and Nanoengineering; Dan V. Nicolau; Ed., 2002.

9. Duy K Pham, Elena P Ivanova, Jonathan P Wright, Piotr A Grodzinski, Ralf Lenigk, Dan V Nicolau Surface characterization of oligonucleotides immobilized on polymer surfaces Proc. SPIE Vol. 4937, 115-124, Biomedical Applications of Micro- and Nanoengineering; Dan V. Nicolau; Ed., 2002.

10. Dan V Nicolau Patterning biomolecules and cells: an upside-down microlithography (INVITED PAPER). Proc. SPIE Vol. 4690, p. 11-17, Advances in Resist Technology and Processing XIX; Theodore H. Fedynyshyn; Ed., 2002.

11. Gregory S Watson, Jolanta A Blach, Dan V Nicolau, Sverre Myhra Radiation patterning of P(tBuMA-co-MMA) thin films for biosensor applications: characterization by scanning probe microscopy Proc. SPIE Vol. 4626, 58-68, Biomedical Nanotechnology Architectures and Applications; Darryl J. Bornhop,

David A. Dunn, Raymond P. Mariella, Jr., Catherine J. Murphy, Dan V. Nicolau, Shuming Nie, Michelle Palmer, Ramesh Raghavachari; Eds., 2002

12. Dan V Nicolau, Dan V Nicolau Database comprising biomolecular descriptors relevant to protein adsorption on microarray surfaces. Proc. SPIE Vol. 4626, 109-115, Biomedical Nanotechnology Architectures and Applications; Darryl J. Bornhop, David A. Dunn, Raymond P. Mariella, Jr., Catherine J. Murphy, Dan V. Nicolau, Shuming Nie, Michelle Palmer, Ramesh Raghavachari; Eds., 2002.

13. Dan V Nicolau, Dan V Nicolau Model of protein adsorption to solid surfaces from solution Proc. SPIE Vol. 4626, 1-8, Biomedical Nanotechnology Architectures and Applications; Darryl J. Bornhop, David A. Dunn, Raymond P. Mariella, Jr., Catherine J. Murphy, Dan V. Nicolau, Shuming Nie, Michelle Palmer, Ramesh Raghavachari; Eds., 2002.

14. Jonathan P Wright, Chitladda Mahanivong, Duy K Pham, Dan V Nicolau, K Suyama, Masamitsu Shirai, Masahiro Tsunooka Computer-controlled laser ablation: a novel tool for biomolecular patterning Proc. SPIE Vol. 4590, 345-353, BioMEMS and Smart Nanostructures; Laszlo B. Kish, Erol C. Harvey, William B. Spillman, Jr.; Eds., 2001.

15. Jinan Cao, Duy K Pham, Livia Tonge, Dan V Nicolau Computation of the true surface properties of proteins on the Connolly molecular surface Proc. SPIE Vol. 4590, p. 273-279, BioMEMS and Smart Nanostructures; Laszlo B. Kish, Erol C. Harvey, William B. Spillman, Jr.; Eds., 2001.

16. Jinan Cao, Duy K Pham, Livia Tonge, Dan V Nicolau Simulation of the force-distance curves of atomic force microscopy for proteins by the Connolly surface approach. Proc. SPIE Vol. 4590, p. 187-194, BioMEMS and Smart Nanostructures; Laszlo B. Kish, Erol C. Harvey, William B. Spillman, Jr.; Eds., 2001.

17. Livia Tonge, Jinan Cao, Duy K Pham, Jonathan P Wright, Erol C Harvey, Dan V Nicolau Scaling relationship between laser ablation rates and polymer descriptors for polymers used in microfluidics. Proc. SPIE Vol. 4590, p. 179-186, BioMEMS and Smart Nanostructures; Laszlo B. Kish, Erol C. Harvey, William B. Spillman, Jr.; Eds., 2001.